EXPERIMENTAL INVESTIGATION FOR THE EFFECTS OF THE CORE GEOMETRY ON THE OPTIMUM ACID FLUX IN CARBONATE ACIDIZING

A Thesis

by

XIAO JIN

Submitted to the Office of Graduate and Professional Studies of
Texas A&M University
in partial fulfillment of the requirements for the degree of

MASTER OF SCIENCE

Chair of Committee,	Ding Zhu
Committee Members,	A. Daniel Hill
	Michael Pope
Head of Department,	A. Daniel Hill

December 2013

Major Subject: Petroleum Engineering

ABSTRACT

Previous matrix acidizing experimental research showed that there exists an optimum acid interstitial velocity ($V_{i\text{-}opt}$) that results in the minimum volume of acid used while providing the best stimulation results. There are already several upscaling models that translate experimental results into field conditions. By finding the optimum core geometry to use for matrix acidizing experiments, a great amount of time and money will be saved in selecting the correct size core for future experimental work. Laboratory experiments have already indicated that the optimum acid interstitial velocity can be independent of the core length when the core length is long enough.

In this thesis, further core flood experiments were done using four inches diameter cores that varied in length. The lengths of the cores are 4 inches, 6 inches, and 8 inches long. The acid concentration used for these experiments was 15 wt% HCl. A pressure drop plot was created as the acid penetrates through the core sample. By looking at the pressure drop plot, the start of acid penetration, the early stages of wormhole competition, the later stages of a dominant wormhole forming, and the time when the acid breaks through the core can all be recorded.

Theoretical works were done to correlate experimental results with previously published work. It can be concluded that when the core reaches a certain length, the optimum interstitial velocity becomes independent of the core length due to the dominant wormhole being formed. Also, when the core length reaches a certain value, the optimum acid injection rate is independent of the core radius given that the core

radius is large enough to comprise the early effects of wormhole competition. One inch diameter cores should never be used because it only shows the dominant wormhole being formed.

ACKNOWLEDGEMENTS

I would like to thank my committee chair, Dr. Ding Zhu, as well as my committee members, Dr. Hill and Dr. Pope, for their continuous support throughout my time here as a Master of Science student here at Texas A&M. Additionally, I would like to thank Shell for providing the cores that are needed for part of my thesis. Finally, I would like to thank my family and fraternity brothers in pushing me through the final stretch of this program.

NOMENCLATURE

N_{AC}	Acid Capacity Number
β	Acid Dissolving Power
t	Acid Injection Time
C	Concentration
A	Core Cross-sectional Area, cm^2
d	Core Diameter, cm
L	Core Length, cm
M	Core Mass, g
ρ	Density, g/cm^3
γ	Fluid Loss Limited Wormholing
q	Injection Rate, bbl/min
V_i	Interstitial Velocity
h	Interval length, ft
N	Number of Dominant Wormholes per 2D Plane
$V_{i,opt}$	Optimum Interstitial Velocity, cm/min
$PV_{bt,opt}$	Optimum Pore Volumes to Breakthrough, Dimensionless
ϕ	Porosity, dimensionless
PV_{bt}	Pore Volume to Breakthrough, Dimensionless
V	Volume, cm^3
V_{wh}	Wormhole Growth Rate, cm/min
L_{wh}	Wormhole Length in Linear Flow, L, ft

r_{wh} Wormhole Penetration Length, ft

TABLE OF CONTENTS

Page

Page

LIST OF FIGURES

Page

Page

LIST OF TABLES

Page

CHAPTER I

INTRODUCTION

1.1 Problem Statement

Matrix acidizing is a widely used technique to improve well performance, especially in carbonate reservoirs. Acid is injected into the formation to create long flow channels called wormholes. These wormholes bypass damaged zones around the well to greatly reduce the skin factor and increase productivity of the well. The main design parameters of an acid stimulation treatment include injection rate, acid volume and type, and concentration of the acid.

There have been many publications for the study of carbonate acidizing treatment design. Coreflood experiments are the simplest way to study the effect of these parameters on stimulation results. Lab results indicate that there exists an optimum acid injection rate which gives the best stimulation result with the least amount of acid. The resulting acid injection rate is then scaled up for field designs using various wormhole models.

The dimensions of experimental cores can affect the coreflood experimental results. It is known that under identical conditions, larger diameter cores result in a lower optimum interstitial velocity and a longer core results in a higher one. Studies also have shown that the optimum interstitial velocity is independent of the core length when the core is long enough. If a critical core length at which the optimum interstitial

velocity becomes independent of the core radius can be determined, the effect of core dimension on the coreflooding result can be eliminated.

1.2 Background and Literature Review

The structure of wormhole in acid stimulation in carbonate reservoirs is an important parameter when optimizing stimulation design. For carbonate reservoirs, the primary acid used is hydrochloric acid (HCl), which reacts and dissolves the minerals near the wellbore to increase the permeability. The dissolution of carbonate rocks with HCl includes two reactions. For calcite

$$CaCO_3 + 2HCL \rightarrow CaCl_2 + CO_2 + H_2O \quad \text{..... (1.1)}$$

and for dolomite

$$4HCl + CaMG(CO_3)_2 \rightarrow CaCl_2 + MgCl_2 + 2CO_2 + 2H_2O \quad \text{..... (1.2)}$$

Many researchers have conducted experiments relating to the optimum conditions for carbonate acidizing. Hoefner and Fogler (1987) studied the effect of injection and dissolution rates on carbonate acidizing by conducting laboratory experiments with limestone and dolomite samples. Hoefner and Fogler (1989) then further developed their research and discovered that a high dissolution rate increases stimulation efficiency, but a rate that is very high decreases the stimulation efficiency. Hung et al. (1989) created a model of wormhole growth and competition that accounted for the decrease in acid concentration as it propagates through the wormhole because of diffusion and fluid loss out of the wormhole wall. This model agrees with Hoefner and Fogler's findings that states the efficiency of the stimulation depends on the dissolution rate of the carbonate.

Daccord et al. (1989) presented a wormhole propagation model based on the dissolution patterns created by injecting water into plaster. He concluded that for a highly reactive system, an optimum flow rate does exist. Wang et al. (1993) conducted linear corefloods using carbonates and confirmed with Daccord's simulation that an optimum injection rate does exist in highly reaction systems. The optimum injection rate varies with rock mineralogy, acid concentration, and reaction temperature. This leads to many future studies in finding the optimum injection rate by conducting coreflooding experiments under various conditions.

Frick et al. (1994) conducted radial coreflood experiments to compare with linear coreflood experiments to observe differences in scaling up to field conditions. The experimental results revealed that the optimum flow rate predicted from experiments is significantly lower than the one observed in the field practices. He concluded that radial flow experiments were more difficult to perform but did provide a better indication of field conditions. **Figure 1.1** shows a plot of breakthrough pore volume versus interstitial velocity from different experimental studies. It clearly shows that the optimal condition exist for all tests. Mostofizadeh and Economides (1994) developed a method to upscale the lab results to field conditions. Through the development of the method, he found also that permeability and the optimum injection rate are strongly related. Hill et al. (1995) presented the volumetric model. The volumetric model simply uses a concept of breakthrough pore volume to estimate the distance of wormhole growth into the formation. To apply the model, breakthrough pore volume has to be obtained from a different source (mostly from lab experiment). A

constant wormhole growth rate is assumed, which leads to increased error as wormhole grows.

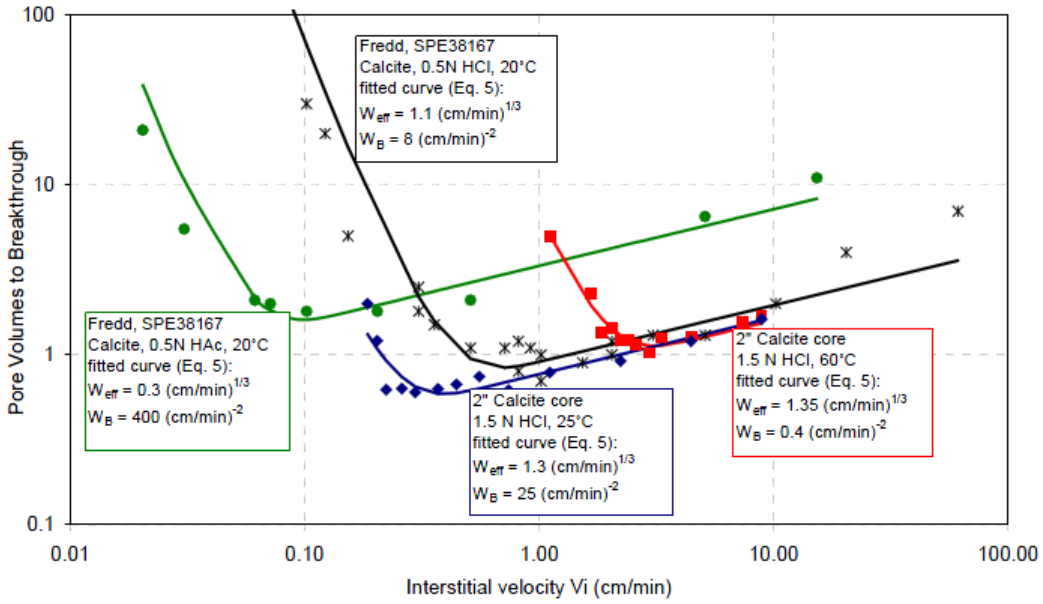

Figure 1.1: Pore Volume to Breakthrough (From Buijse and Glasbergen, 2005)

A semiempirical model was presented by Buijse and Glasbergen (2005)**.** This model relates the pore volume of breakthrough to the wormhole propagation rate shown in **Figure 1.1.** Only two values, the interstitial velocity and the corresponding pore volume to breakthrough is needed. Both values are found through coreflood experiments. Furui et al. (2010) concluded that the velocity at the tip of the propagation wormholes drives the wormhole propagation rate. This results in a higher interstitial velocity than the average interstitial velocity used in the Buijse and Glasbergen model. Just like the Buijse and Glasbergen model, Furui's model also requires the optimum interstitial velocity and the corresponding pore volume to breakthrough.

Many experimental studies have been conducted in order to obtain the optimum interstitial velocity and the corresponding pore volume to breakthrough. By using the Buijse and Glasbergen model, Talbot and Gdanski (2008) fitted the data from Bazin (2001), Wang et al. (1993), Smits (2001), and Fredd and Fogler (1999). The data fit using Bazin's experimental data is shown in **Figure 1.2.** Buijse (2000) concluded that under identical conditions, the core sizes of experiments affect the scale up from linear coreflood to field operations.

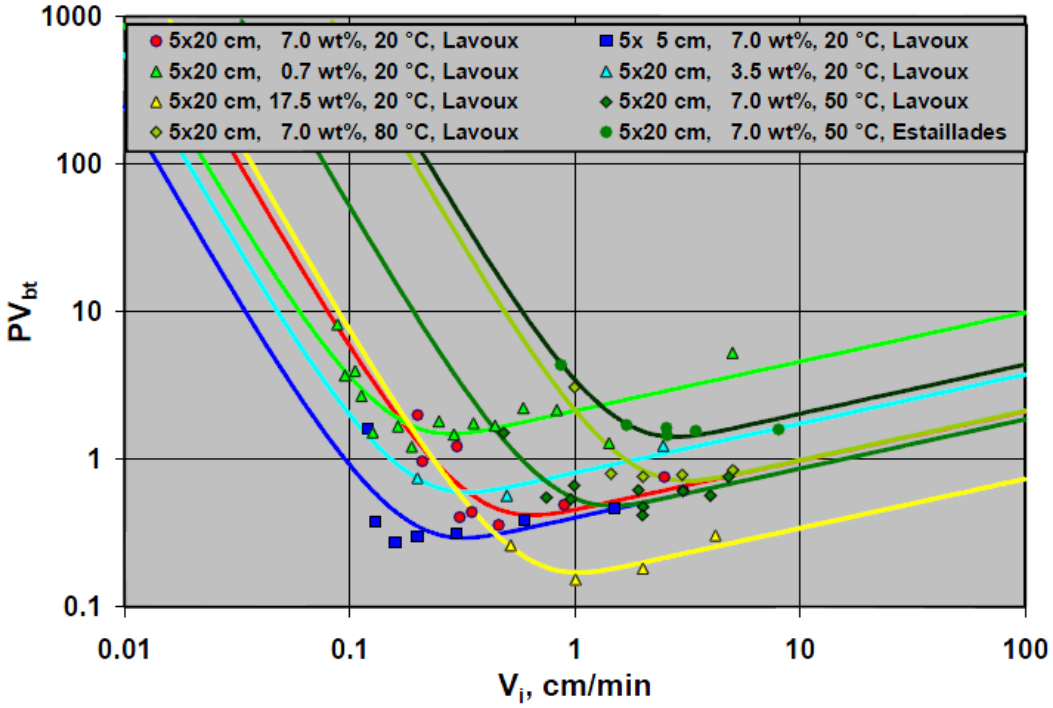

Figure 1.2: Data from Bazin (From Talbot and Gdanski, 2008)

1.3 Objectives of This Study

In this research the relationship between the core geometry and the optimum interstitial velocity is studied. Once the optimum interstitial velocity is found to remain

constant when the core length reaches a certain value and becomes independent of the core radius, future research should be able to choose the correct core length depending on core diameter.

Indiana limestone is chosen for this study due to its homogeneity so the results are not affected by rock heterogeneity. Three series of experiments were run. The series include core length of 4 inches, 6 inches, and 8 inches. The diameter of all of the cores is 4 inches. The results are then compared with previous results that also used Indiana limestone for 1 inch and 1.5 inches core diameters. Observation of the experiments will help to address the effect of core radius on wormhole development.

CHAPTER II

EXPERIMENTAL APPARATUS AND PROCEDURE

This chapter provides a summary of the apparatus used in matrix acidizing experiments. The equipment was designed and assembled by Elizabeth Grabski (2012) and modified in order to successfully run the experiment for this study.

2.1 Overall Schematic

The schematic of the equipment shown below is provided below (Ghosh, 2013):

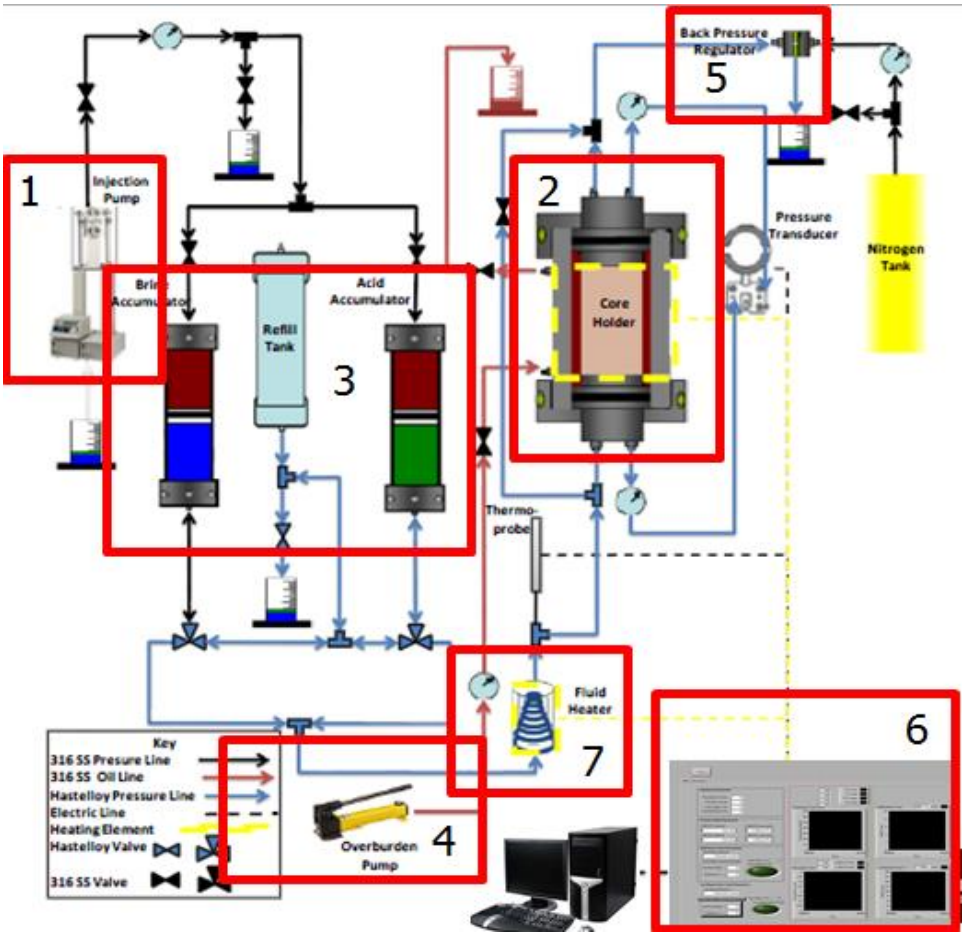

Figure 2.1: Matrix Acidizing Equipment Schematic (From Ghosh, 2013)

The functions of the individual components used in the equipment apparatus will be explained in the following sections:

1. injection pump
2. core holder
3. hydraulic accumulators
4. overburden pump
5. backpressure regulator
6. data acquisition system
7. fluid heater
8. back pressure regulator

2.1.1 Injection Pump

A Teledyne ISCO high pressure injection pump used in the experiments is shown in the schematic chart **(Figure 2.1)** labeled as part 1**.** The injection pump includes two accumulators that hold the injecting brine. The pump is a continuous flow dual pump that can be pressurized up to a maximum of 7,500 psi. Each of the pump accumulators can hold up to 260 mL of liquid. The advantage of having dual accumulators is that as long as the reservoir contains water, the pump can keep injecting until the accumulator is empty without stopping to refill the injection pump during the experiment. The injection pump is designed to have a maximum injection rate of 107 mL/min, but in order to have continuous flow the injection rate cannot exceed 50 mL/min. This is due to the maximum refill rate being 100 mL/min and that the refill rate needs to be at least twice as much as the injection rate for continuous flow. Water is used as the reservoir fluid as

the current equipment does not allow hydraulic oil to be used due to the higher viscosity of the oil. The procedure steps for operating the syringe pump are provided by Grabski (2012).

2.1.2 Core Holder

The core holder holds the core samples and the spacers that together must be equal to twenty inches in length. The core holder is shown in the schematic chart (**Figure 2.1**) labeled as part 2. Spacers are used to fill up the empty space in the core holder after the core is in place. Three parts make up the core holder: the inlet cap, outlet cap, and the main body.

2.1.3 Hydraulic Accumulators

Two hydraulic accumulators are used throughout the experiment. The accumulators are shown in the schematic chart (**Figure 2.1**) labeled as part 3. One stores the brine and the other stores the acid. The hydraulic accumulator is a metal container that contains a piston that separates the injection fluid and the fluid that is to be injected into the core holder. During the experiment, the injection pump pushes the water into the upper chamber of the accumulator and the piston pushes the stored liquid into the core holder. The accumulator that does not store acid is made from stainless steel and does not corrode from brine. The accumulator that stores the acid is made of Hastelloy material. Each accumulator has a capacity of 1 liter, thus restricting the water and acid that can be used in one experiment to 1 liter only.

2.1.4 Hydraulic Pump

The hydraulic pump is a hand pump that is used to apply confining pressure between the Viton sleeve and metal cylinder of the core holder. The pump is shown in the schematic chart in **Figure 2.1** labeled as part 4. Motor oil is stored inside the hydraulic pump and pumped into the core holder. The confining pressure is usually kept at a steady 500 psi above the injecting pressure for 2 reasons. The first reason is the minimum confining pressure limit is used to make sure that the fluid passes through the bypass and not through the core holder. The second reason is that the upper confining pressure limit prevents the fracture of the core due to excessive confining pressure between the Viton sleeve and the core metal cylinder of the core holder.

2.1.5 Backpressure Regulator

The backpressure regulator is used to hold pressure at the outlet of the core and is labeled as part 5 in the schematic chart in **Figure 2.1**. The backpressure requirement during the experiment is maintained constantly at a pressure of at least 1,000 psi to prevent carbon dioxide from forming in the liquid during acid injection. For laboratory experiments with samples that are cored from downhole, the backpressure may be much higher in order to simulate the reservoir pressure.

2.1.6 Data Acquisition System

The data acquisition system includes the Labview software that is specifically designed to measure the pressure drop from the top of the core holder to the bottom of the core holder, a pressure transducer is used to detect the pressure change, and a NI

circuit board that acts as a medium to transfer data from the transducer to the Labview software. This system is labeled in the schematic charge in **Figure 2.1** as part 6.

2.1.7 Heating System

The matrix acidizing experimental apparatus is designed to be able to run high temperature experiments. The heater is shown in **Figure 2.1** and labeled part 7. Heating tape is used to increase the temperature of the tubing and core holder when it is wrapped around the equipment. In order to heat the equipment to the desired temperature quickly, fiber glass is used to insulate the core holder and pipe. Additionally, thermocouples are attached to the core holder and also at certain spots on the heater in order to make sure that the desired temperature is achieved before acid injection. It is important to note that heating up the core holder and tubing could take many hours.

2.2 Experimental Procedure

A summary of a matrix acidizing experiment is summarized as follow:

1. Dry core samples and measure the dry weight
2. Saturate the core for at least 6 hours in a vacuum pump and measure the wet weight
3. Calculate the porosity of the core and insert the core into the core holder with enough spacers to fill the entire length of the core holder
4. Fill the water accumulator and the acid accumulator with the correct injection fluids

5. Start injecting with the injection pump at the desired flow rate and then apply at least 1,000 psi of back pressure
6. Increase the confining pressure so that the difference between the confining pressure is always 500 psi more than the injection pressure
7. Keep injecting brine into the system until the entire system is pressurized.
8. Close the bypass valve so the brine goes through the core and permeability can be calculated using Darcy's law after the pressure drop become stabilized.
9. Open the valve of the acid accumulator and close the valves of the brine accumulator in one quick motion. Timer should start now.
10. Once the acid breakthrough occurs (noticeable by looking at the pressure drop on the pressure transducer and the pressure drop plot on the Labview software) stop the timer
11. Close the acid accumulator valves and open the water accumulator valves to flush the system.
12. Flushing the system is very important right after the experiment because corrosion inhibitors are not used.
13. When the flow of liquid coming out of the core holder is no longer acidic, (this may take several refills in the water accumulator depending on the core holder) the experiment can be stopped and the core can be removed from the core holder.

2.2.1 Core Preparation

The experiments involve 4 inch diameter cores at varying length of 4 inches, 6 inches, and 8 inches. The cores are numbered before each experiment for the later data analysis. Permanent marker is highly recommended so core saturation and coreflooding does not remove the numbers. The core is then put into an oven for at least 2 hours. Once the core is dry take it out of the oven to measure the dry weight. The core is then saturated by using a vacuum pump. It should take no more than 6 hours to fully saturate the core. Once the core is fully saturated the wet weight is measured using the same scale. Porosity can then be calculated with the dry weight and wet weight.

2.2.2 Injection Fluid Preparation and Refilling

The water used for the experiments is regular tap water. The acid used has a weight percent of 36.5%. The desired concentration for these experiments is 15 wt% HCl.

To make 15 wt% HCl the following equation is used:

$$Volume\ HCL = \frac{Wt_{required} * \rho_{required}}{Wt_{given} * \rho_{given}} \quad \ldots\ldots\ldots\ldots\ldots\ldots\ldots\ldots\ldots\ldots\ldots\ldots\ldots\ldots (2.1)$$

The density of the HCl with 36.5 wt% is 1.18 g/mL and the density of 15 wt% HCl is 1.07 g/mL. Plugging the density and weight percentage 373.05 mL of HCl and 626.95 mL of water for 1L of 15 wt% HCl is needed. It is convenient to always make 1L of 15 wt % HCl because the acid accumulator can hold 1L. It also allows running several experiments in succession and prevents failure of experiments due to running out of acid in low flow rate experiments.

A picture with the accumulator, shown in **Figure 2.2**, includes the refill tank, injection pump, and valves.

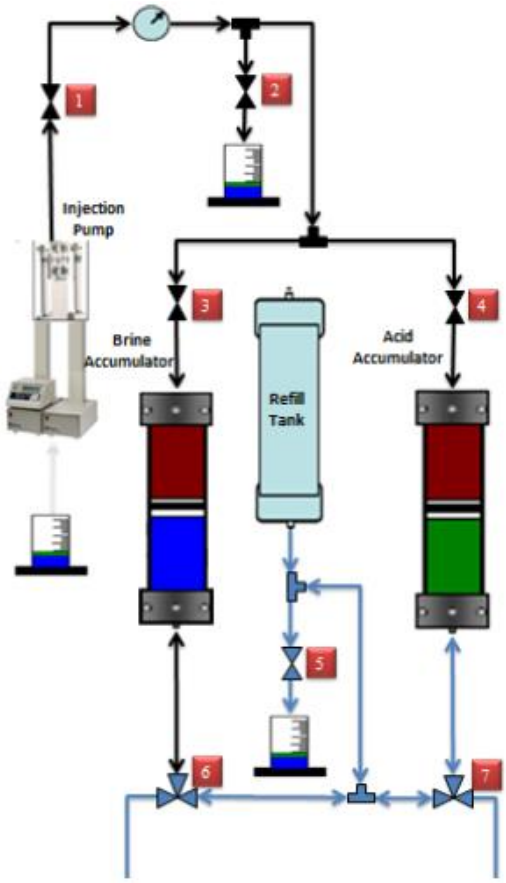

Figure 2.2: Accumulator Scheme (From Ghosh, 2013)

Before starting the experiment it is important to make sure that the brine and acid accumulators are both empty. This is done by following these steps:

1. Open only valves 1 and 2 and inject at a flow rate of 25 mL to check for air. When a steady flow comes out of valve number 2 there should be no air in the injection pump.

2. In order to remove all previous brine in the brine accumulator close valves 2, 4 and 7 completely. Then open valves 1, 3, 5, and open valve 6 in a way that the brine previously stored in the accumulator only goes through valve 5.
3. In order to remove all previous acid in the acid accumulator close valves 3 and 6 completely. Then open valves 1, 4, 5, and open valve 7 in a way that the acid previously stored in the accumulator only go through valve 5.

When the pressure shoots up on the injection pump it means that the piston is already pushed to the bottom and that all the fluids in the accumulators were pushed out. The next step is to fill the acid accumulator with 1,000 mL of acid. This is done in the following steps:

1. Prepare 1,000 mL of acid in a precision beaker so it's easier to accurately measure the volume of brine and acid mixed together to form 15 wt % HCl.
2. Close all valves numbered on the picture completely except for valve 5 to check that there is no liquid in the refill tank.
3. Close valve 5 and pour the acid into the refill tank carefully.
4. The refill tank is connected to an air pump attached to the wall. Open valves 2, 4 and make sure that valve 7 is opened in a way that the liquid only travel through valve 4. Valves 1, 3, 6, and 5 should be closed.
5. Close the top of the refill tank and open the air pump slowly. This should push the acid at a steady rate into the acid accumulator.
6. It is important to close valve 7 when there is still a small amount of acid in the refill tank. This makes sure that no air goes into the acid accumulator.

7. When the acid accumulator is filled as much as possible close all the valves except for 5. The remaining acid should go into the beaker at valve 5. Now the refill tank is empty.

The refill tank needs to be cleaned before filling brine into the brine accumulator. This is done by filling up the entire refill tank with water and letting the water run into the beaker at valve 5 with the help of the air pump until the pH of the brine coming out of valve 5 is nonacidic. The steps to refill the accumulator with brine are done in the following steps:

1. Prepare 1,000 mL of brine in a precision beaker.
2. Close all valves numbered on the picture completely except for valve 5 to check that there is no liquid in the refill tank.
3. Close valve 5 and pore the brine into the refill tank carefully.
4. The refill tank is connected to an air pump attached to the wall. Open valves 2, 3 and make sure that valve 6 is opened in a way that the liquid only travel through valve 4. Valves 1, 4, 7, and 5 should be closed.
5. Close the top of the refill tank and open the air pump slowly. This should push the acid at a steady rate into the brine accumulator.
6. It is important to close valve 6 when there is still a small amount of brine in the refill tank. This makes sure that no air goes into the brine accumulator.
7. When the brine accumulator is filled as much as possible close all the valves except for 5. The remaining brine should go into the beaker at valve 5. Now the refill tank is empty.

Both the acid accumulator and the brine accumulator should be now filled with nearly 1,000 mL of injection fluids.

2.2.3 Core Holder Setup

The core holder consists of an inlet cap, out let cap, and the Hastelloy cylinder. The position of the 4 inch core holder should be left at a horizontal position in between experiments. Since the 4 inch core holder is always attached in the current apparatus it is very easy to rotate it into a vertical position after the core and spacers are inserted. This is done by removing the pin that is holding the core horizontally and inserting the pin again when the core holder is vertical. In order for the Viton sleeve to not break due to confining pressure, there must be exactly 20 inches in length of core and spacers inside the core holder. The core should be at the inlet (bottom of the core holder) and the rest of the space in the core holder is filled with spacers all the way to the outlet. The inlet and outlet caps are then attached. A cap sealer is tightened around the outlet cap. This prevents the outlet cap from pushing out due to the confining pressure inside the core holder. The schematic for setting up the connections to the core holder is shown in **Figure 2.3**. From this figure we observe that the outlet and inlet both have 2 connections. The outlet and inlet is connected by tubing through a pressure transducer. The transducer measures the pressure drop across the core holder. With the use of a 3-way valve, the outlet is connected with a bypass shown as tubing #1, and the nitrogen tank with tubing #2. The 3-way valve at the inlet connects the bypass and the fluid injection tubing. The bypass tube (tubing #1) is important because it allows the injection fluid to bypass the core if there is confining pressure inside the core holder already. This

is used to fill the spacer with fluid so there is no air in the system. Without the bypass, injecting fluid through the core holder and through the Indiana limestone in order to fill up the spacer would take much more time because fluid have to through the core first before filling the spacers.

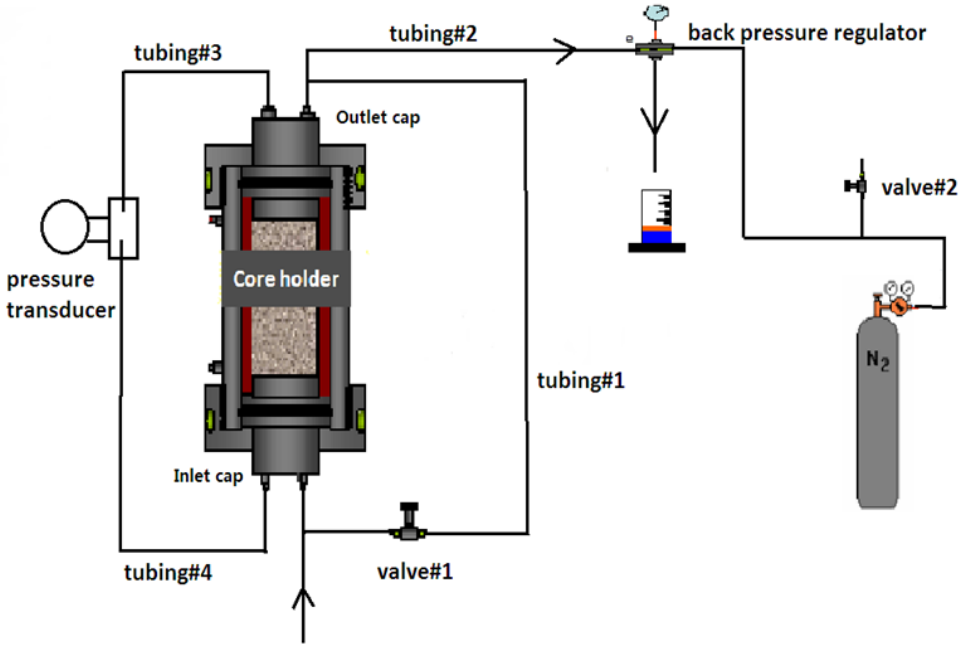

Figure 2.3: Core Holder Connection Schematics (From Dong, 2012)

2.2.4 Injection Procedure

Before starting injection, Labview should be open and a new file should have been created. Labview records the pressure drop over time which allows us to observe when acid breakthrough the core.

On the side of the core holder there are two additional connections. Both are for the use of controlling the confining pressure inside the system. The top connection is connected to a closable that allows the release of confining pressure slowly if needed.

This is important because too much confining pressure can damage the core. The valves are also used at the end of the experiment to slowly release confining pressure at a similar rate with the release of backpressure through the valve attached to the nitrogen tank to prevent unnecessary fracturing of the cores that were already acidized.

The hydraulic pump is attached to the bottom valve. Once the core holder is set up and the injection fluids are in the accumulator confining pressure can be applied. Pump hydraulic oil into the core holder until the confining pressure reaches 500 psi. Leave the bypass valve open and inject brine through the system by opening both sides of the brine accumulator. Note that during injection, the bottom valve of the acid accumulator valve should be closed but the top must be open. This is to prevent the pressure drop suddenly dropping to 0 psi when the water accumulator is closed during acid injection. Brine should come out through the backpressure regulator. Now open the nitrogen tank until the backpressure reaches 1,000 psi. This is required because it will prevent carbon dioxide from being formed during acidizing. The brine that was flowing out of the backpressure regulatory should stop and go into the core holder to fill in the spacers, because the backpressure is higher than the confining pressure. The injection pressure (shown on the injection pump) rises when the spacers are filled with water. The injection pressure should keep going up and eventually match up with the backpressure. At that point the fluid should come out of the backpressure regulator‘s exist. Note that it is important to pump more hydraulic oil once the injection pressure goes up so that the confining pressure is constantly 500 psi higher than the injection pressure.

Once the backpressure is equal to the injection pressure and brine is flowing out at a steady rate close the bypass valve. This forces the brine to go through the core holder and create a pressure drop. The pressure drop is shown on Labview. Once the pressure drop is stabilized for a short period of time acid injection can began.

The correct procedure for acid injection using **Figure 2.3** is as follows:

1. Adjust flow rate corresponding the desired interstitial velocity
2. Open valve #7, start timer
3. Close valve #6

After starting acid injection observe the pressure drop plot on Labview. Acid breakthrough happens when the pressure drop suddenly drops and then becomes stabilized. This is shown and discussed in detail in Chapter 3. Stop the timer as soon as breakthrough occurs and record the final time.

2.2.5 Post Flush

Post flush using brine is done to clean the acid out of the system. This is done by closing vale #7 and opening valve #6 to run the cleaning fluid through the system. Once the fluid coming out of the backpressure regulator exist is no longer acidic the core can be safely removed from the core holder without causing corrosion damage to the tubings. At this point if there is still acid remaining inside the acid accumulator it needs to be pushed out using the method described in **Section 2.2.2**. It is also important to run brine at least once through the acid accumulator to prevent corrosion in the 3-way valve underneath the acid accumulator.

CHAPTER III

EXPERIMENTAL RESULTS

The experimental result includes the pressure and injection rate data recorded during experiments, and the calculated pore volume to breakthrough. The data is then used to generate wormhole efficiency curves (PV_{BT} vs. interstitial velocity).

3.1 Data Recording

Recording the data is just as important as properly running the experiment. In this chapter a sample data sheet is shown that should be followed for any matrix acidizing experiment. Pressure drop plots are also shown in this chapter so typical variations with experiments running at high temperature and using heterogeneous cores can be explained.

Table 3.1: Data Recording in Matrix Acidizing Experiment

1	Core#	4 x 4 M1	5	Date	November 27, 2012
	Core diameter	4 inch			
	Core length	4 inch	6	Acid Coreflooding	
				Temperature	75 °F
2	Porosity Measurement				
	Weight (Dry)	1835.9 g	7	Depth	N/A ft
	Weight (Sat)	1962.9 g		Solubility	100 %
	Porosity	15.42%			
	Pore Volume	127 cm^3	8	Acid Injection Rate	12.5 cc/min
			9	Interstitial Velocity	1.00 cm/min
3	Permeability Measurement		10	Volume of Pipe between Core and Acid tank	5.86 cm^3
	Injection Rate	12.5 cc/min			
	Pressure Differential	69 psi			
	Permeability	5.56 md	11	Time for Acid to Get the Core	28.1 seconds
4	Acid Formulation	15 wt% HCl	12	Time for Acid Injection	203 seconds
	Water	626.95 cm^3			
	HCl (37 wt%)	373.05 cm^3	13	Pore Volume Break Through	0.29 Pore volume

1. The core was labeled as M1. The diameter and length are properly recorded for future calculations.
2. The dry weight is measured after the core is put into an oven and completely dried. The wet weight is measured after the core has been saturated at full vacuum pressure for at least 6 hours long. Equations are given below to calculate porosity:

$$V_{bulk} = A * L \quad \text{(3.1)}$$

$$V_{pore} = \frac{(m_{saturated} - m_{dry})}{\rho_{water}} \quad \text{(3.2)}$$

$$\phi = \frac{V_{pore}}{V_{bulk}} * 100\% \quad \text{(3.3)}$$

Porosity is obtained with these equations using the data presented in **Table 3.1**:

$$\phi = \frac{(m_{saturated} - m_{dry})/\rho_{water}}{(2.54 * D)^2 * \frac{\pi}{4} * (2.54 * L)} * 100\% \quad \text{(3.4)}$$

$$\phi = \frac{\frac{(1962.9 - 1835.9)g}{1g/cm^3}}{(2.54\ \frac{cm}{inch} * 4\ inches)^2 * \frac{\pi}{4} * (2.54\ \frac{cm}{inch} * 4\ inches)} * 100\%$$

$$= 15.42\% \quad \text{(3.5)}$$

The equation to calculate pore volume is given as:

$$Pore\ Volume = \phi * \frac{\pi}{4} * \left(Diameter * 2.54\ \frac{cm}{inch}\right)^2 * (Length * 2.54\ \frac{cm}{inch}) \quad \ldots\ldots\ldots\ldots\ldots\ldots\ldots\ldots (3.6)$$

Pore volume is obtained with this equation using the data presented in **Table 3.1**:

$$Pore\ Volume = 0.1542 * \frac{\pi}{4} * \left(4\ inches * 2.54\ \frac{cm}{inch}\right)^2 * \left(4\ inches * 2.54\ \frac{cm}{inch}\right)$$

$$= 127\ cm^3 \quad \ldots\ldots\ldots\ldots\ldots\ldots\ldots\ldots\ldots\ldots (3.7)$$

3. The injection rate used is dependent on the selected interstitial velocity for the experiment. It is not a calculated value. The pressure differential is determined from the pressure drop. The pressure drop stabilizes at 69 psi before injection in this example.

$$k = \frac{96.43 * 4 * Q * L * \mu}{\pi * D^2 * \Delta p} \quad \ldots\ldots\ldots\ldots\ldots\ldots\ldots\ldots\ldots\ldots (3.8)$$

Permeability is obtained with this equation using the data presented in **Table 3.1**:

$$k = \frac{96.43 * 4\ inches * 12.5\ \frac{cm^3}{min} * 4\ inches * 1\ cp}{\pi * (4\ in)^2 * 69\ psi}$$

$$= 5.56\ md \quad \ldots\ldots\ldots\ldots\ldots\ldots\ldots\ldots\ldots\ldots (3.9)$$

4. The acid formulation was discussed earlier for 15 wt% HCl.

$$Volume\ HCL = \frac{Wt_{required} * \rho_{required}}{Wt_{given} * \rho_{given}} \quad \ldots\ldots\ldots\ldots\ldots\ldots\ldots\ldots\ldots (3.10)$$

$$Volume\ HCL = \frac{0.15\ wt\ \% *\ 1.07\ g/mL}{0.3646\ \% *\ 1.18\ g/mL}$$

$$= 373.05\ mL \quad \ldots\ldots\ldots\ldots\ldots\ldots\ldots\ldots\ldots\ldots\ldots\ldots\ldots\ldots \quad (3.11)$$

$$Volume\ Brine = 1{,}000\ mL - Volume\ HCL = 1{,}000\ mL - 373{,}05\ mL$$

$$= 626.95\ mL \quad \ldots\ldots\ldots\ldots\ldots\ldots\ldots\ldots\ldots\ldots\ldots\ldots\ldots\ldots \quad (3.12)$$

5. Keeping track of the date of experiment is optional, but it might be important for future references.
6. 4 inches diameter cores are run under temperature of 75 degree Fahrenheit.
7. Since the experimental core samples are homogenous Indiana limestone, it will be 100% acid soluble in HCl.
8. The acid injection rate is selected based on the desired interstitial velocity. For each group of experiment that shares the same radius and core length, different acid injection rate should be selected so that the interstitial velocity covers all the flow regions. In **Figure 3.1** three different wormhole morphologies are shown. The top wormhole casting is caused by low injection rate, the middle one caused by selecting a near optimum injection rate, and the last one is caused by high injection rate.

Figure 3.1: Wormhole Morphologies Using Different Injection Rates

9. Interstitial velocity is the velocity of the injection fluid being injected through the pore space cross sectional area of the core.

$$v_i = \frac{Q}{(\frac{\pi}{4} * (2.54 * D)^2 * \ \phi)} \ldots \ldots \ldots \ldots \ldots \ldots \ldots \ldots \ldots \ldots \ldots \ldots \ldots \ldots \ldots \ldots \ldots . . \ldots \ldots \ldots \ldots . (3.13)$$

Interstitial velocity is obtained with this equation using the data presented in **Table 3.1**:

$$v_i = \frac{12.5 \ cm^3/min}{(\frac{\pi}{4} * \left(2.54 \ \frac{cm}{inch} * 4 \ inches\right)^2 * \ .1542)} = 1.00 \ cm/min \ \ldots \ldots \ldots . . \ldots . (3.14)$$

10. The volume of pipe between core and acid tank needs to be calculated in order to calculate the time for the acid to get the core. Without subtracting this time from the total acid injection time, the time for acid injection is not accurate. The equation to calculate this is given as:

$$V = L * 2.54\ \frac{cm}{inch}$$

$$* \frac{\pi}{4}\ ((tubing\ inner\ diameter) * 2.54\ \frac{cm}{\text{min}})^2 \quad \ldots\ldots\ldots\ldots\ldots\ldots (3.15)$$

The volume of pipe is obtained with this equation using the data presented in **Table 3.1**:

$$V = 518\ in * 2.54\ \frac{cm}{in} * \frac{\pi}{4}\ (0.12)^2$$

$$= 5.86\ cm^3 \quad \ldots\ldots\ldots\ldots\ldots\ldots\ldots\ldots\ldots\ldots\ldots\ldots\ldots\ldots\ldots\ldots\ldots\ldots\ldots\ldots (3.16)$$

The tubing inner diameter can be measured using a caliper.

11. The time for acid to get to the core is given by the following equation:

$$Time\ for\ acid\ to\ reach\ the\ core$$

$$= \frac{V}{Q} \quad \ldots\ldots\ldots\ldots\ldots\ldots\ldots\ldots\ldots\ldots\ldots\ldots\ldots\ldots\ldots\ldots\ldots\ldots\ldots\ldots\ldots\ldots\ldots\ldots\ldots\ldots (3.17)$$

The time for acid to reach the core is obtained with this equation using the data presented in **Table 3.1**:

$$Time\ for\ acid\ to\ reach\ the\ core = \frac{5.86\ mL}{12.5\ \frac{mL}{min}} * 60\ \frac{sec}{min}$$

$$= 28.1\ sec \quad \ldots\ldots\ldots\ldots\ldots\ldots\ldots\ldots\ldots\ldots\ldots\ldots\ldots\ldots\ldots\ldots\ldots\ldots\ldots\ldots\ldots\ldots\ldots\ldots\ldots\ldots (3.18)$$

12. Time for acid injection is timed using a stop watch.
13. Pore volume to breakthrough relates acid flow rate with time and pore volume. The lowest pore volume to breakthrough would give the dominant wormhole, thus allowing the engineer to determine the optimum injection rate to use. The equation is given by:

$$PVBT = \frac{(Time\ for\ acid\ injection - time\ for\ acid\ to\ reach\ core) * Q}{PV} \quad \ldots\ldots\ldots\ldots (3.19)$$

PVBT is obtained with this equation using the data presented in **Table 3.1**:

$$PVBT = \frac{(203\ sec - 28.1\ sec) * 12.5\ \frac{mL}{min}}{60\ \frac{sec}{min} * 127\ mL}$$

$$= 0.29\ pore\ volumes \quad \ldots\ldots\ldots\ldots\ldots\ldots\ldots\ldots\ldots\ldots\ldots\ldots\ldots\ldots\ldots\ldots\ldots\ldots (3.20)$$

3.2 Example of Standard Pressure Drop Data Plot Example

The pressure drop versus time plot shows many important things regarding the experiment. The simplest information the plot gives is when the acid breakthrough the core. **Figure 3.2** is an example of the three pressure drop sections during acid injection.

Section 1 occurs between the beginning of acid injection and when the acid reaches the core. The plot does not tell us exactly where acid injection started because the stabilized pressure drop does not change until acid starts to break through the core sample.

Section 2 is in between when the acid reaches the core and when the acid breakthrough the core. The sharp drop is caused by the acid creating the wormhole that eventually reach breakthrough at the outlet of the core.

Section 3 is similar to section 1 in that a flat pressure drop is observed again. The negligible pressure drop confirms that acid have broken through the core.

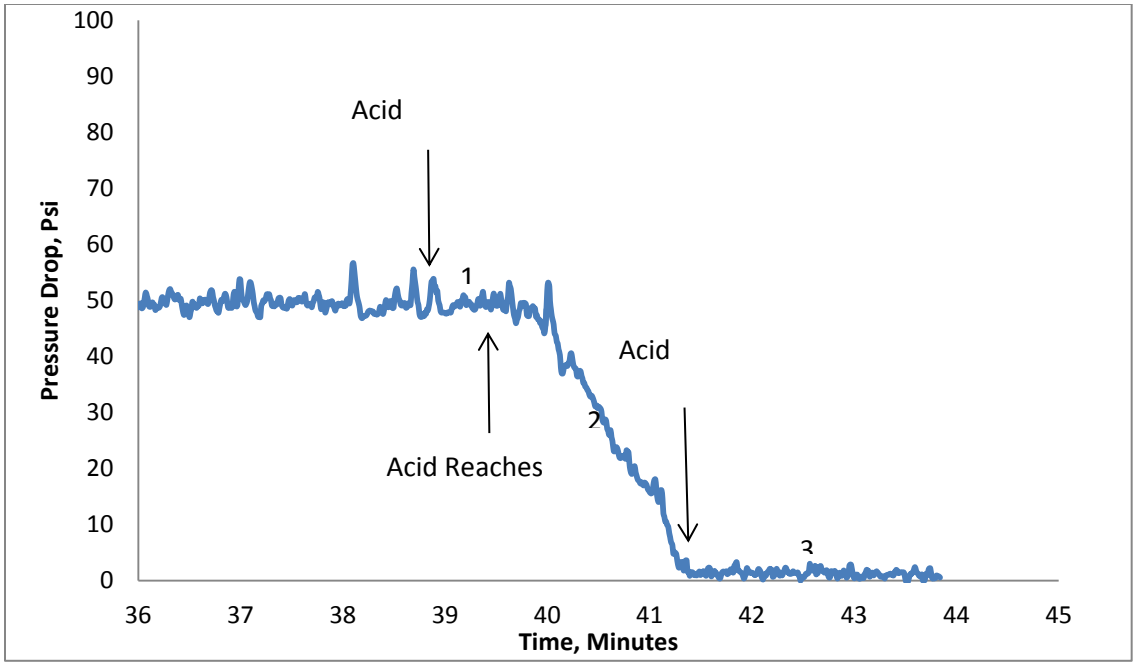

Figure 3.2: Pressure Drop Plot Example

3.3 Pressure Drop Plot Variations

Variations from the standard plot are mainly due to core heterogeneity. Some pressure plots with variations are presented in this section. **Figure 3.3** shows a pressure drop plot with significant difference from standard pressure drop behavior. The pressure drop increased suddenly and then becomes flat. This is caused by the pressure drop exceeding the max pressure that the pressure transducer can read. When this happens lower the flow rate so that the pressure drop falls below the maximum pressure allowed by the transducer. Do not inject acid if stabilized pressure drop is not obtained.

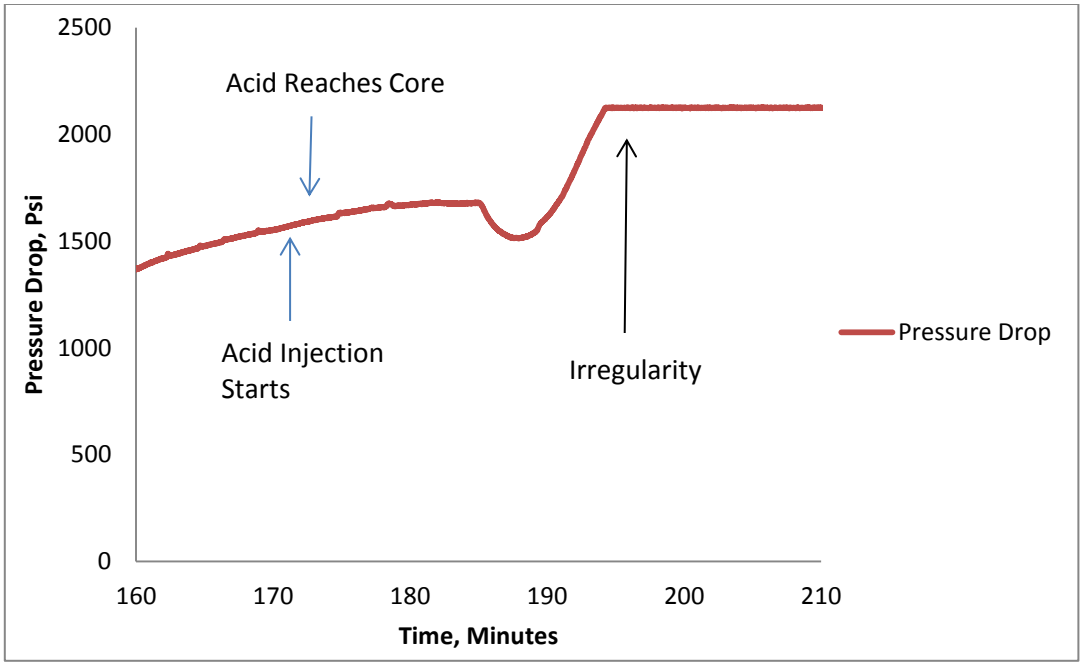

Figure 3.3: Pressure Drop Too High for Pressure Transducer

The type of irregularity shown in **Figure 3.4** is caused by two possibilities:

1. At high temperature heterogeneous cores always seem to result in a rise in pressure drop when acid reaches the core. This does not necessarily mean that there is an experimental error. This high pressure drop is most likely due to acid dissolving the calcite surrounding pieces of rocks that are not reactive with the acid. The rocks that are not reactive with HCl would then plug up the core, preventing the acid from easily penetrating through the core sections that are made up of calcite.
2. If this is seen in a homogenous core, then this is more likely is connected to an experimental error. This may be caused by decreasing of the backpressure because the nitrogen tank is not connected correctly. If this is the cause, it is

necessary to restart the experiment and make sure that the nitrogen tank is opened correctly so that it is keeping the backpressure constant.

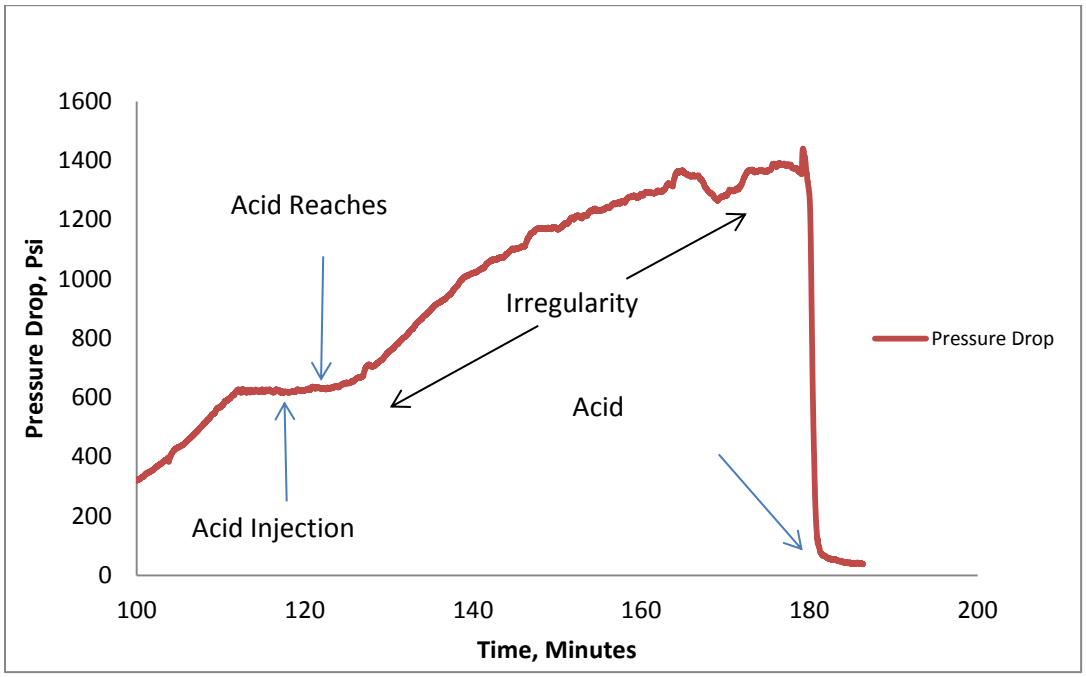

Figure 3.4: Pressure Drop in Low Solubility Cores

In **Figure 3.5,** the pressure drop after the acid started to penetrate the core is not steadily decreasingly as shown in **Figure 3.2**. This is most likely due to a low injection rate, which leads to undissolved carbon dioxide. By increasing the back pressure, this issue should be removed. If this were to happen in an experiment, the best solution would be to do the same experiment again under a higher backpressure.

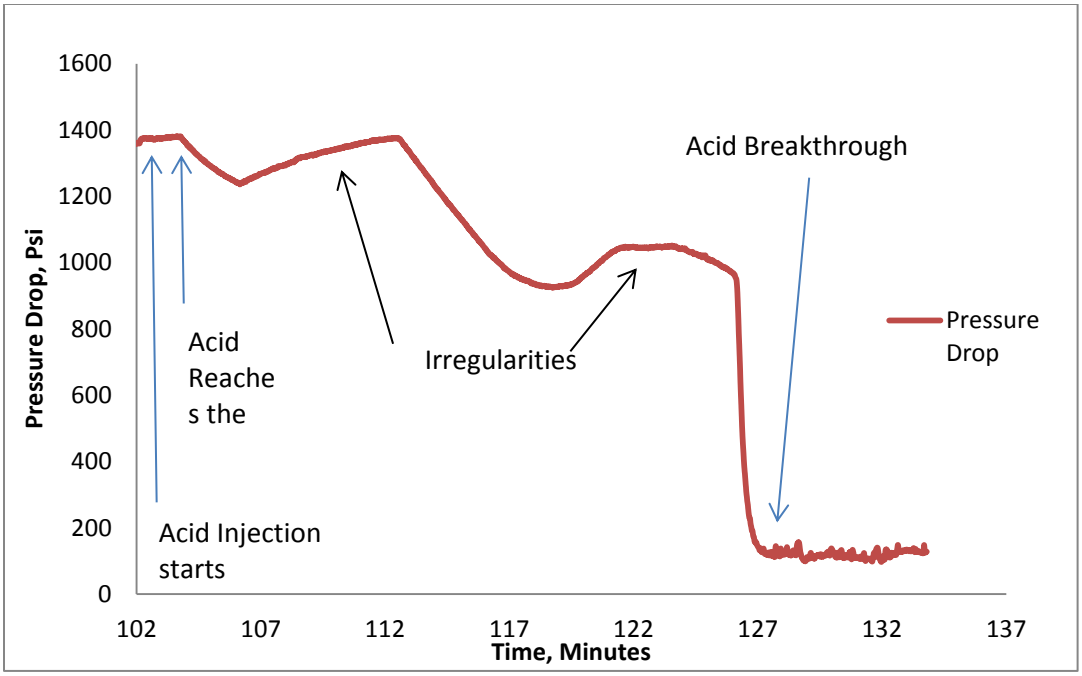

Figure 3.5: Fluctuations in Pressure Drop During Acidizing

Figure 3.6 shows two additional plots. One is the core holder temperature and the other is the fluid temperature. It is important to show these two plots in a high temperature experiment to validate that the experiment was indeed conducted at the required temperature. The core holder and the fluid temperature are stable enough to be acceptable.

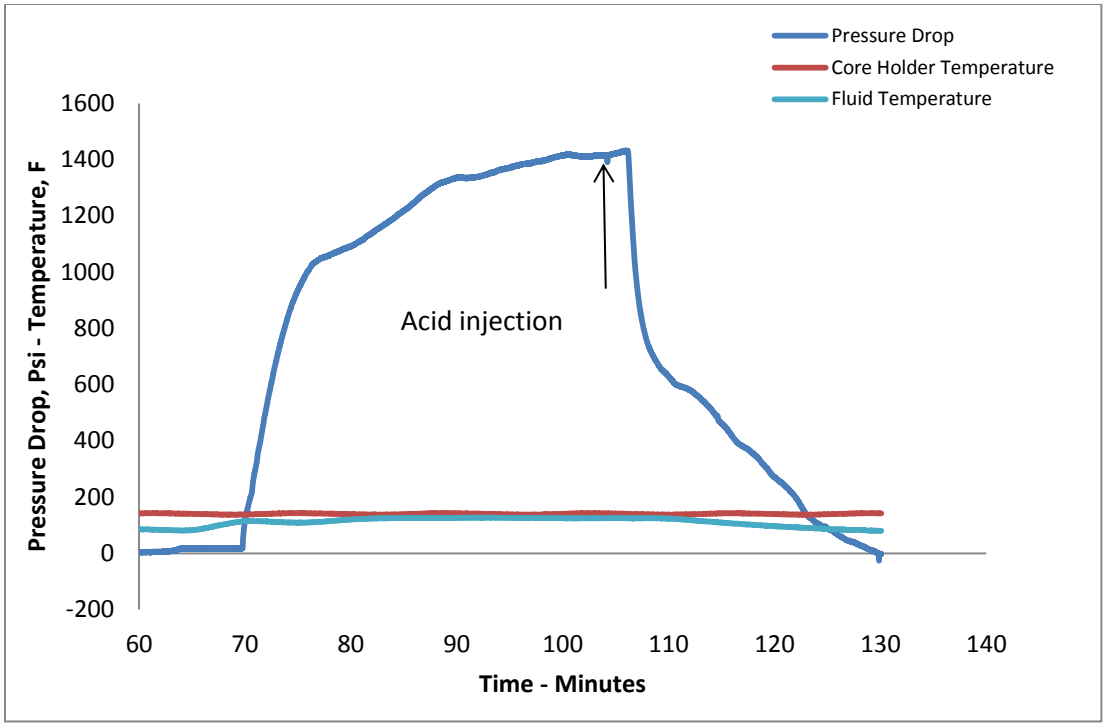

Figure 3.6: Pressure Drop at High Temperature

\

CHAPTER IV

THE EFFECT OF CORE GEOMETRY ON WORMHOLING

The focus of this research involves the study of the effect of core geometry on the optimum interstitial velocity. The experimental data is fitted using the Buijse-Glasbergen model. After the data is fitted, observations are made on how the length and radius of the core affect the interstitial velocity. Studying how the geometry of the core affect the optimum interstitial velocity is a small part of the goal of creating a model that allows the calculation of the optimum interstitial velocity without conducting experiments in the future.

4.1 Buijse and Glasbergen Model

Buijse and Glasbergen (2005) developed a semiempirical model to predict the pore volume breakthrough and wormhole propagation rate. This model is used here for the curve fitting of all the experimental data that has been gathered.

The Buijse and Glasbergen semiempirical model can be described with the equations below:

$$PV_{bt} = \frac{V_i^{1/3}}{W_{eff*}B(V_i)} \quad \text{(4.1)}$$

$$W_{eff} = \frac{V_{i-opt}^{1/3}}{PV_{bt-opt}} \quad \text{(4.2)}$$

$$B(V_i) = [1 - \exp(-W_B * V_i^2)]^2 \quad \text{(4.3)}$$

$$W_B = \frac{4}{V_{i-opt}^2} \quad \ldots \quad (4.4)$$

PV_{bt-opt} and V_{i-opt} both can be obtained through experimental results. The four equations shown above can be combined into 1 equation shown below:

$$PV_{bt} = PV_{bt-opt}\left(\frac{V_i}{V_{i-opt}}\right)^{\frac{1}{3}}\{1 - \exp\left[-4\left(\frac{V_i}{V_{i-opt}}\right)^2\right]\}^{-2} = f(V_i) \quad \ldots \quad (4.5)$$

By using the least square method, (shown in the equation below), the experimental data can be fitted. The *n* is the amount of experimental data points and the residue *J* should be minimized. Proper PV_{bt-opt} and V_{i-opt} values are selected to minimize the residue.

$$J = \sum_{i}^{n}[PV_{bt}^{i} - f(V_i^i)]^2 \quad \ldots \quad (4.6)$$

4.2 The Effect of Core Length on the Optimum Interstitial Velocity

In order to study the effect of core length on the optimum interstitial velocity, experiments were conducted using cores of different core length for each given radius. **Table 4.1** shows the number of cores that was matrix acidized for each set of length and diameter. There are a total of 44 cores that were run for the 1 inch diameter, 44 cores for the 1.5 inches diameter, and 16 cores that were run for the 4 inches diameter. The amount of cores that were run was dependent on how many points was required to have points in all three regions of the interstitial velocity versus pore volume to breakthrough curve.

Table 4.1: Core Samples Size Distribution

Length, Inches	Amount (1 Inch Diameter)	Amount (1.5 Inches Diameter)	Amount (4 Inches Diameter)
1	**12**	**--------**	**--------**
2	**13**	**--------**	**--------**
4	**9**	**11**	**8**
6	**10**	**12**	**4**
8	**--------**	**11**	**4**
10	**--------**	**10**	**--------**

The core samples used were Indiana Limestone samples due the homogeneity of the rock. **Table 4.2** shows the average porosity and average permeability for each set of core geometry. Notice that the average porosity ranges from 14% to 16% and the average permeability ranges from 2.9 md to 8.1 md.

Using the Buijse-Glasbergen model, the interstitial velocity and pore volume to breakthrough data points were fitted. The 1 inch diameter core experimental data fits are shown in **Figure 4.1,** the 1.5 inches diameter core data fits shown in **Figure 4.2**, and the 4 inches diameter data fits are shown in **Figure 4.3**. The experimental results conducted using the 1 inch and 1.5 inches diameter cores are from Dong (2012). The 4 inches diameter core samples were matrix acidized for this research study.

Table 4.2: Average Porosity and Average Permeability

Length, Inches	Average Prosity, Average Permeability (1.5 Inches Diameter)	Average Prosity, Average Permeability (1.5 Inches Diameter)	Average Prosity, Average Permeability (1.5 Inches Diameter)
1	15%, 2.9 md	--------	--------
2	14%, 4.3 md	--------	--------
4	14%, 5.5 md	15%, 5.4 md	15%, 3.9 md
6	15%, 7.9 md	15%, 6.8 md	14%, 5.7 md
8	--------	15%, 5.9 md	15%, 3.0 md
10	--------	16%, 8.1 md	--------

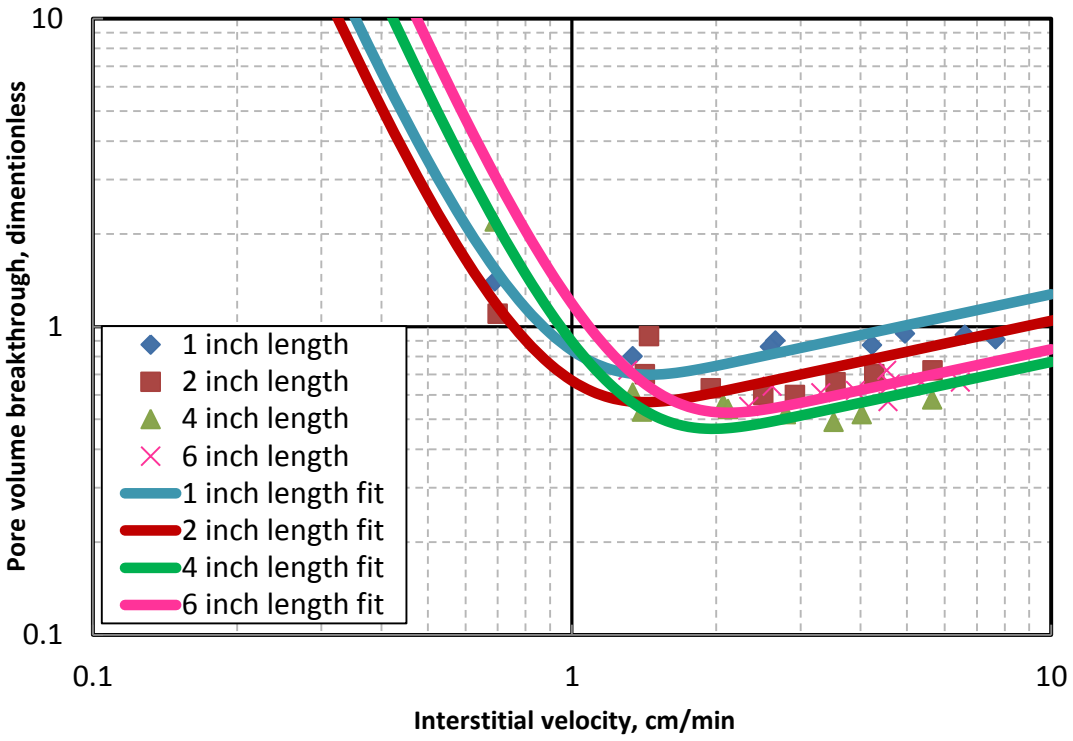

Figure 4.1: 1 Inch Core Diameter Data Fits (From Dong, 2012)

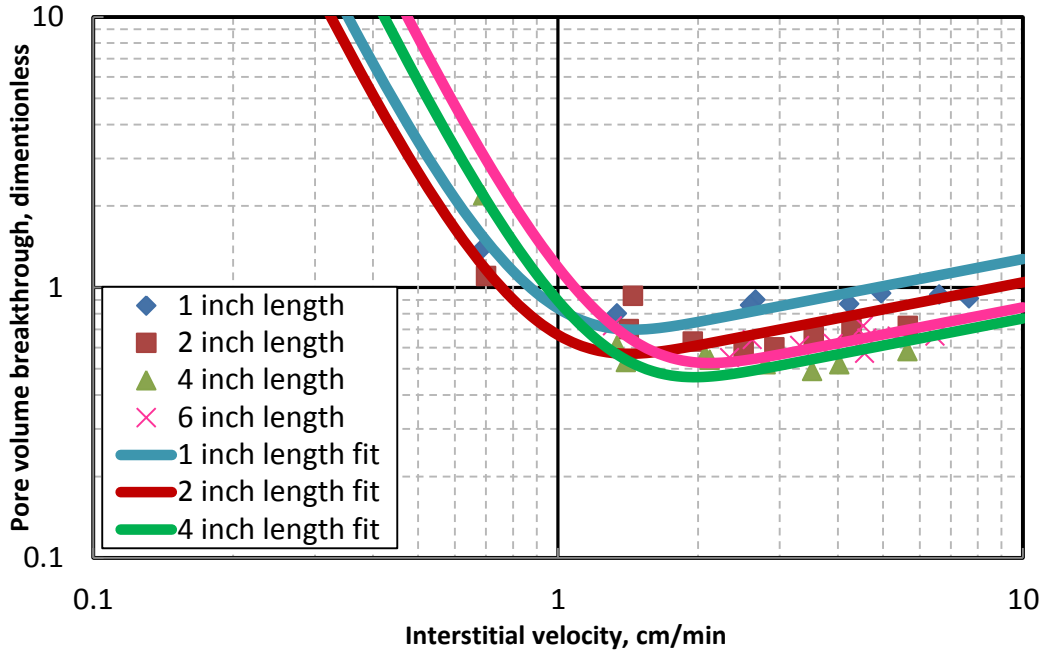

Figure 4.2: 1.5 Inches Core Diameter Data Fits (From Dong, 2012)

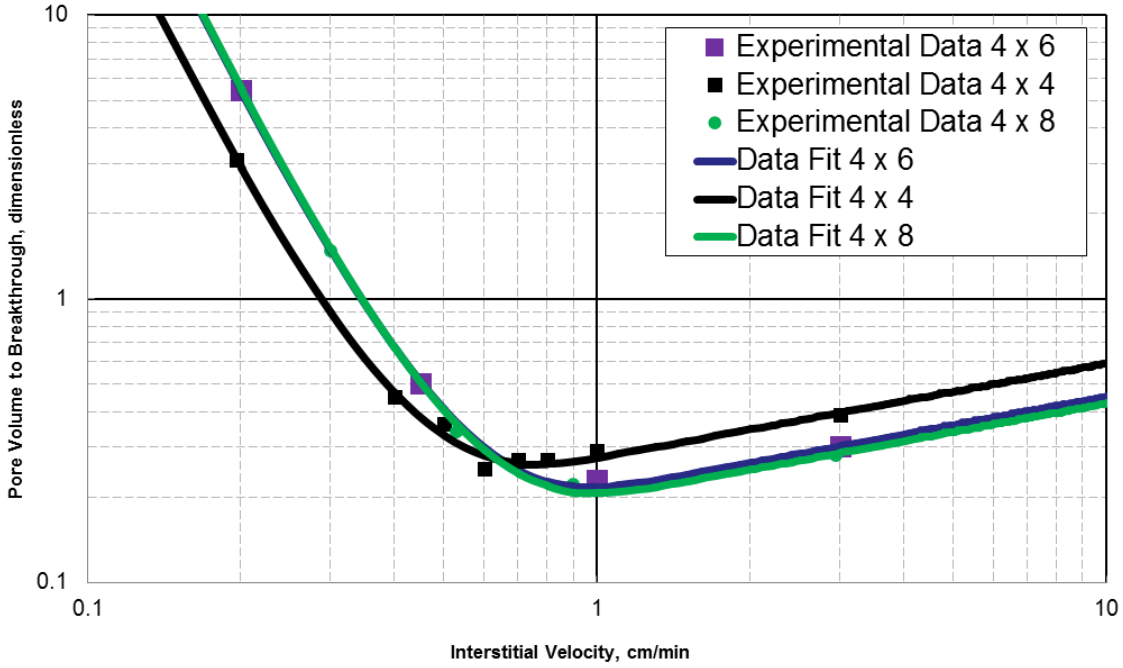

Figure 4.3: 4 Inches Core Diameter Data Fits

Table 4.3 shows the optimum interstitial velocity obtained for each set of core geometries.

Table 4.3: Optimum Interstitial Velocity of Experimental Results

Length, Inches	V_i, opt, cm/min (1 Inch Diameter)	V_i, opt, cm/min (1.5 Inches Diameter)	V_i, opt, cm/min (4 Inches Diameter)
1	**1.4763**	**--------**	**--------**
2	**1.4465**	**--------**	**--------**
4	**2.0003**	**1.6228**	**0.77069**
6	**2.1631**	**1.9630**	**0.98199**
8	**--------**	**1.9837**	**1.00857**
10	**--------**	**1.9600**	**--------**

Dong (2012) concluded that when the length of the core reaches a certain length, it will be independent of the optimum interstitial velocity. This conclusion was made based entirely on looking at the optimum interstitial velocity through the coreflood experiments for the 1 inch and 1.5 inches cores. After conducting experiments with the four inches cores, Dong's conclusion was further proven to be correct. The optimum interstitial velocity was similar after the core reached at least 6 inches in length. In order to gain a better understanding of this conclusion theoretically, it is very important to look at the pressure drop versus time plots for the optimum interstitial velocities. In **Figure 4.4** and **Figure 4.5**, which represent 4 inches diameter by 6 inches length and 4 inches diameter by 8 inches length core geometries respectively, the slope of the pressure drop

changed dramatically during acidizing. Observing **Figure 4.6**, the slope did not change dramatically. This is due to the dominant wormhole forming clearly in the core with 6 inches in length and not clearly in the core with 4 inches in length.

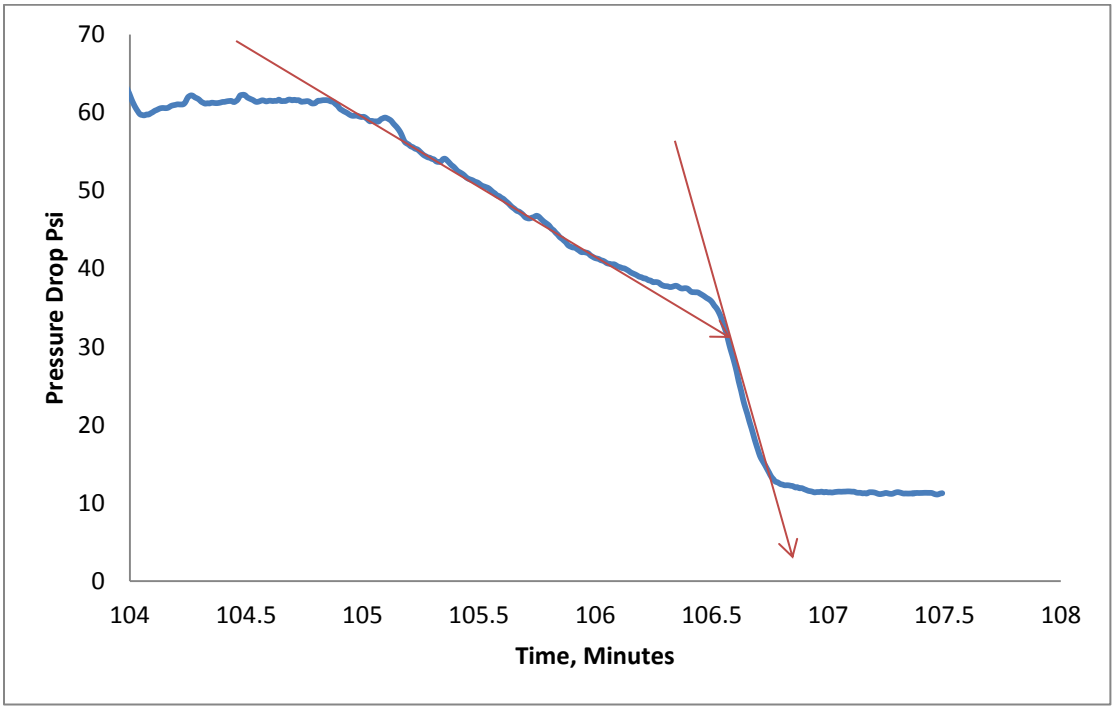

Figure 4.4: Pressure Drop Plot for Optimum Injection Rate for 4 x 6 Core Sample

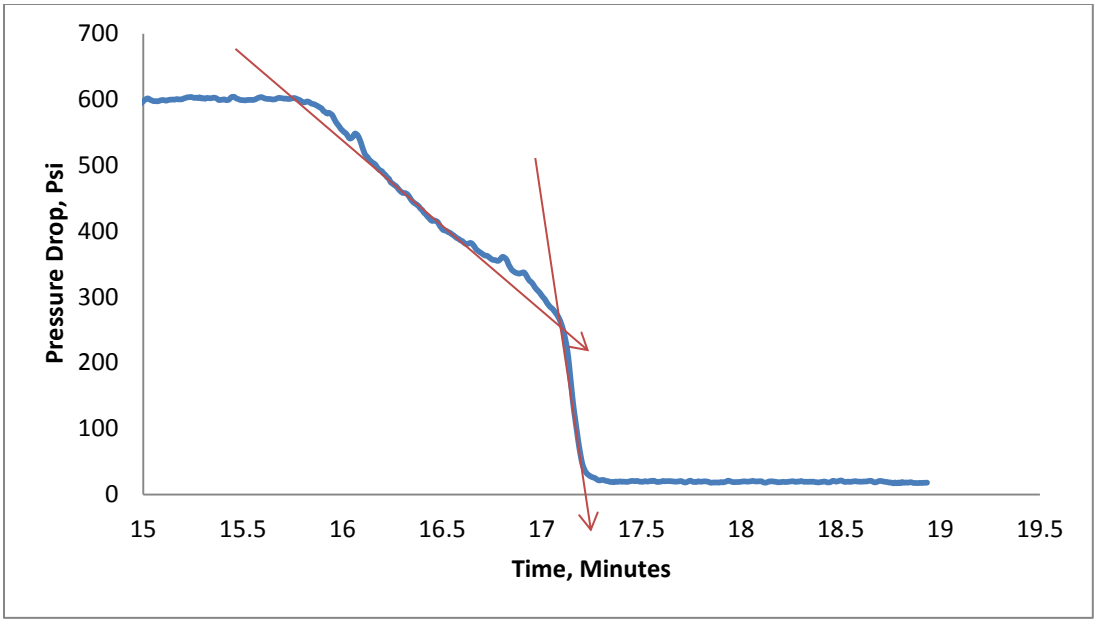

Figure 4.5: Pressure Drop Plot for Optimum Injection Rate for 4 x 8 Core Sample

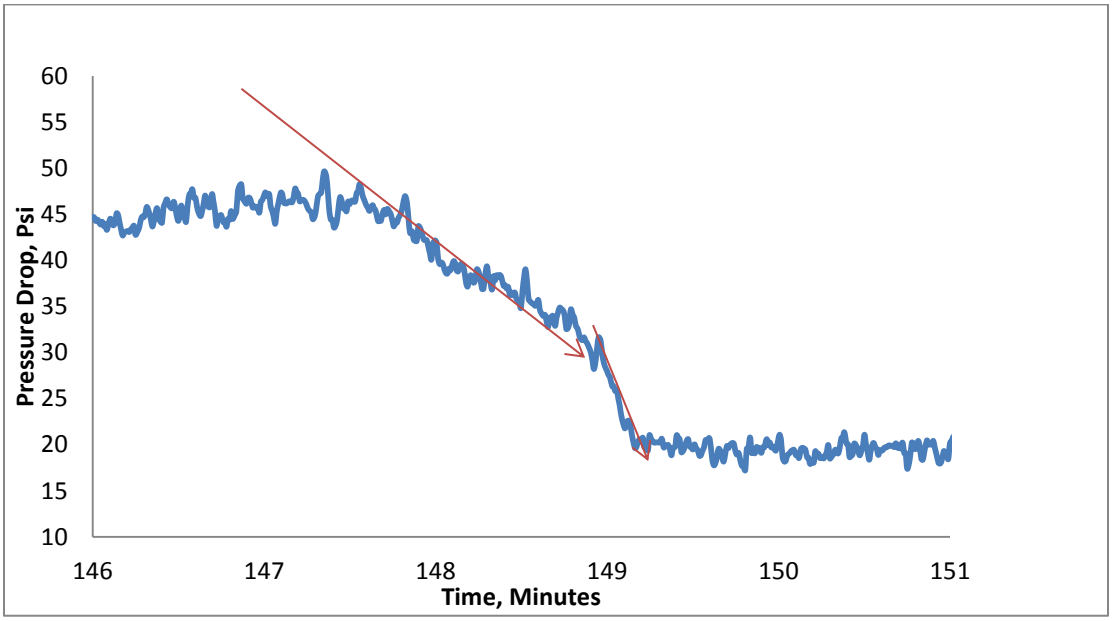

Figure 4.6: Pressure Drop Plot for Nearly Optimum Injection Rate for 4 x 4 Core Sample

In order to further reinforce the observation that a change in the slope as the acid penetrates the core sample represents the dominant wormhole being formed, a CT scan was done for the 4 inches diameter by 8 inches diameter core sample that was matrix acidized at the optimal interstitial velocity. The CT scan is shown in **Figure 4.7**. From this CT scan we observe that there is wormhole competition even if the optimum interstitial velocity was used. The dominant wormhole was not formed until the acid has already penetrated through more than half the core sample. The critical length was 6 inches at which the optimum interstitial velocity becomes nearly constant for the 1.5 inches diameter and 4 inches diameter cores was due to the dominant wormhole not forming until the acid has already penetrated deep into the core sample.

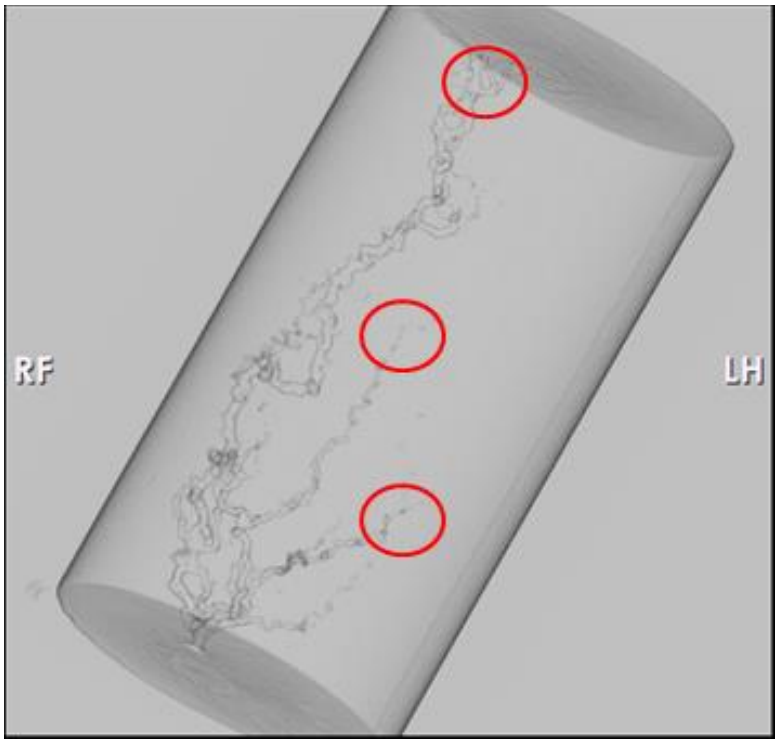

Figure 4.7: CT Scan for 4 Inches by 8 Inches Core Sample with Injection at Optimum Interstitial Velocity

4.3 The Effect of Core Radius on the Optimum Interstitial Velocity

This study concludes that there is a critical length at which the length of the core will be independent of the core radius if the core diameter is at least 1.5 inches. The critical length observed in the study was 6 inches in length for the 1.5 inches diameter and 4 inch diameter cores. The reason that one inch cores have a lower critical length is because it does not accurately represent how the wormhole propagates. **Figure 4.8** shows wormhole castings made by Buijse (2000) to compare the dominant wormhole to its competing wormholes. This shows that when the core diameter is too small, it does not fully represent the actual wormhole propagation during early time.

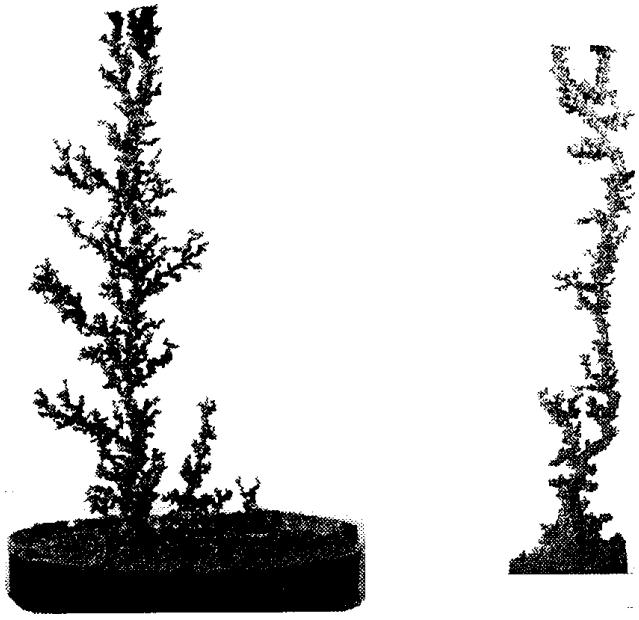

Figure 4.8: 8 cm. Diameter Core (Left) and 2.5 cm. Diameter Core (Right) Wormhole Castings (From Buijse, 2000.)

Using the same core sample shown in **Figure 4.7**, cross sectional images were also taken using the CT scan to look at the wormholes that are formed. In **Figure 4.9** we

have two images. The one on the left is the image of the inlet post-acidizing. The image on the right represents the wormholes that are formed after the acid has penetrated quarter way through the core. In **Figure 4.10**, the left image is when the acid has penetrated half way through the core and the image on the right is when the acid has broken through the core. Looking at the red circles on all images, Buijse conclusion is further reinforced that the core diameter needs to be long enough to show the full extent of wormhole competition. Hence, one inch diameter cores are not recommended for laboratory experiments

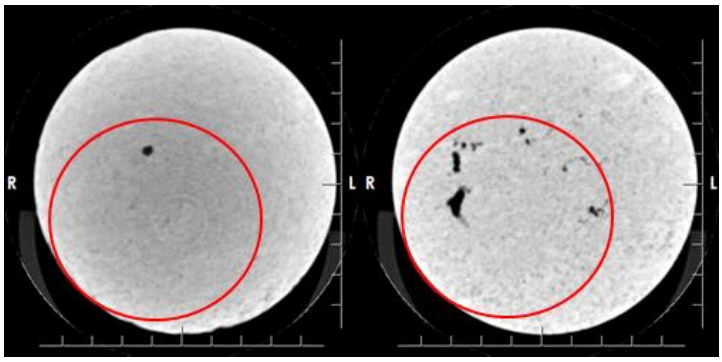

Figure 4.9: CT Scan of Wormhole at Inlet (Left) and Quarter Way into the Core (Right)

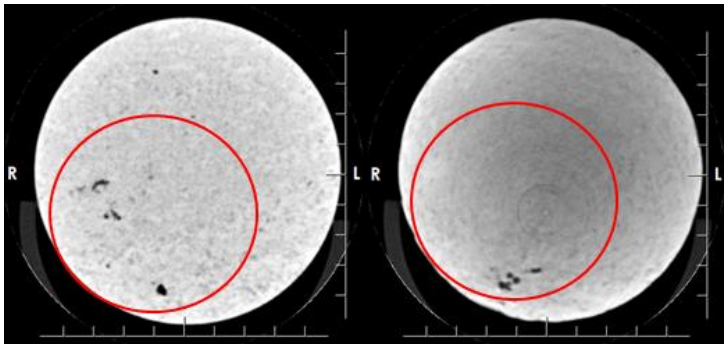

Figure 4.10: CT Scan of Wormhole Half Way into the Core (Left) and Outlet (Right)

CHAPTER V

WORMHOLE MODELS

Three different models are used to scale up experimental data to field conditions:

1. The volumetric method, which predicts the volume of acid required to propagate wormholes a given distance. This model requires an estimation of the average pore volume to breakthrough over the range of fluxes that occurs in the wormhole region. When the acid flux of interest is below the optimum, this model cannot be accurately used because how fast pore volume to breakthrough changes. A more accurate method will be required.
2. Buijse and Glasbergen (2005) presented a semiempirical model that relates the pore volume to breakthrough to the wormhole propagation rate shown in **Figure 1.1**. Only two values, the optimum interstitial velocity and the corresponding pore volume to breakthrough is needed. Both values are found through coreflood experiments.
3. Furui et al. (2010) concluded that the velocity at the tip of the propagation wormholes drives the wormhole propagation rate, which would result in a higher interstitial velocity than the average interstitial velocity used in the Buijse and Glasbergen model. Just like the Buijse and Glasbergen model, Furui's model also requires the optimum interstitial velocity and the corresponding pore volume to breakthrough.

This chapter includes a step-by-step calculation using each of the models with the optimum interstitial velocity and the corresponding pore volume to breakthrough obtained from the experimental results using 4 inches diameter cores. Then all three models are compared by combining their individual wormhole propagation plot into one plot. Both lab data (optimum interstitial velocity and pore volume to breakthrough) and assumed data are used for the calculations.

5.1 Volumetric Model Calculation for Wormhole Propagation

Table 5.1: Assumed Data for Volumetric Model

PVBT	0.25
r_w	0.328 ft
ϕ	0.3
Injection acid volume	100 gal/ft
Injection rate	1 bpm
h	100 ft

Steps to obtain the wormhole propagation plot:

1. In order to obtain the total time needed to have a total injection volume of 100 gal/ft, the following equation is used:

$$total\ injection\ time = \frac{total\ injection\ volume * \frac{1\ ft^3}{7.48\ gal}}{\frac{q}{h} * 5.615\ \frac{ft^3}{bbl}} \ldots\ldots\ldots\ldots\ldots\ldots\ldots\ldots (5.1)$$

$$total\ injection\ time = \frac{100\ \frac{gal}{ft} * \frac{1\ ft^3}{7.48\ gal}}{\frac{1\frac{bbl}{min}}{100\ ft} * 5.615\ \frac{ft^3}{bbl}} = 238.094\ min \quad \ldots\ldots\ldots\ldots\ldots\ldots\ldots\ldots (5.2)$$

2. Choose Δt. Choosing this value is dependent on how accurate the wormhole propagation plot needs to be.
3. At every time step there is a new injection volume. The first time step is calculated at t = 0:

$$current\ injection\ volume = \frac{total\ injection\ volume}{total\ injection\ time} * current\ injection\ time \quad \ldots\ldots\ldots\ldots (5.3)$$

$$current\ injection\ volume = \frac{100\ \frac{gal}{ft}}{238.1\ min} * 0\ \text{min} = 0\ \frac{gal}{ft} \quad \ldots\ldots\ldots\ldots\ldots\ldots\ldots\ldots (5.4)$$

4. At every time step there is a new radius of wormhole propagation. The first time step is calculated as:

$$r_{wh} = \sqrt{r_w^2 + \frac{V}{PV_{bt} * \pi * \phi * h}} \quad \ldots\ldots\ldots\ldots\ldots\ldots\ldots\ldots\ldots\ldots\ldots\ldots\ldots\ldots\ldots\ldots\ldots\ldots\ldots (5.5)$$

$$r_{wh} = \sqrt{(0.328\ ft)^2 + \frac{0\ \frac{gal}{ft} * \frac{ft^3}{7.48\ gal}}{0.25 * \pi * 0.3 * 100\ ft}} = 0.328\ ft \quad \ldots\ldots\ldots\ldots\ldots\ldots\ldots\ldots (5.6)$$

5. At every time step there is a new injection volume. The second time step is calculated at t = 0.1 min:

$$current\ injection\ volume$$

$$= \frac{total\ injection\ volume}{total\ injection\ time} * current\ injection\ time \ldots\ldots\ldots\ldots (5.7)$$

$$current\ injection\ volume$$

$$= \frac{100\ \frac{gal}{ft}}{238.1\ min} * 0.1\ \text{min} = 0.042\ \frac{gal}{ft} \ldots\ldots\ldots\ldots\ldots\ldots\ldots\ldots\ldots\ldots\ldots (5.8)$$

6. At every time step there is a new radius of wormhole propagation. The second time step is calculated as:

$$r_{wh} = \sqrt{r_w^2 + \frac{V}{PV_{bt} * \pi * \phi * h}} \ldots\ldots\ldots\ldots\ldots\ldots\ldots\ldots\ldots\ldots\ldots\ldots\ldots\ldots\ldots\ldots\ldots\ldots\ldots\ldots\ldots\ldots (5.9)$$

$$r_{wh} = \sqrt{(0.328\ ft)^2 + \frac{0.042\ \frac{gal}{ft} * \frac{ft^3}{7.48\ gal}}{0.25 * \pi * 0.3 * 100\ ft}} = 0.36\ ft \ldots\ldots\ldots\ldots\ldots\ldots\ldots (5.10)$$

7. Repeat time steps until total time reaches 238.1 minutes. At 238.1 minutes, 100 gal/ft. is reached in total injection volume. The plot is shown in **Figure 5.1**

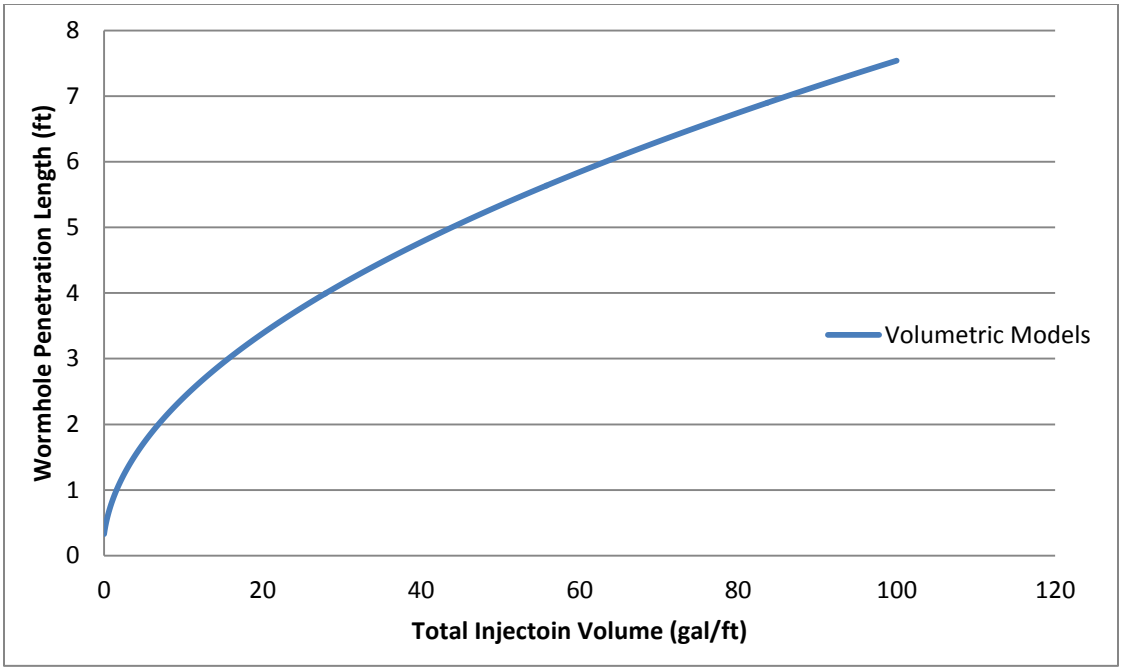

Figure 5.1: Volumetric Model Wormhole Propagation Plot

5.2 Buijse - Glasbergen Model for Wormhole Propagation

The Buijse – Glasbergen model requires an optimum interstitial velocity and its corresponding pore volume to breakthrough. These values are obtained through coreflooding experiments. In the calculations, the values used are from the 4 inches diameter by 4 inch length cores shown in **Table 5.2.**

Table 5.2: Experimental Data Values for Buijse-Glasbergen Model

Optimum Interstitial Velocity, $V_{i,opt}$ (cm/min)	0.77
PV_{bt}	0.25

The assumed values for these calculations are shown in **Table 5.3**

Table 5.3: Assumed Data Values

r_w	0.328 ft
ϕ	0.3
Injection acid volume	100 gal/ft
Injection rate	1 bpm
h	100 ft

Steps to obtain the wormhole propagation plot:

1. In order to obtain total time to have a total injection volume of 100 gal/ft, the following equation is used:

$$total\ injection\ time = \frac{total\ injection\ volume * \frac{1\ ft^3}{7.48\ gal}}{\frac{q}{h} * 5.615\ \frac{ft^3}{bbl}} \ldots\ldots\ldots\ldots\ldots\ldots\ldots (5.11)$$

$$total\ injection\ time = \frac{100\ \frac{gal}{ft} * \frac{1\ ft^3}{7.48\ gal}}{\frac{1\frac{bbl}{min}}{100\ ft} * 5.615\ \frac{ft^3}{bbl}} = 238.094\ min\ \ldots\ldots\ldots\ldots\ldots\ldots (5.12)$$

2. Choose Δt. Choosing this value is dependent on how accurate the wormhole propagation plot needs to be.
3. At every time step there is a new injection volume. The first time step is calculated at t = 0:

$current\ injection\ volume$

$$= \frac{total\ injection\ volume}{total\ injection\ time} * current\ injection\ time \ \dots\dots\dots \ (5.13)$$

$current\ injection\ volume$

$$= \frac{100\ \frac{gal}{ft}}{238.1\ min} * 0\ \text{min} = 0\ \frac{gal}{ft} \ \dots\dots\dots\dots\dots\dots\dots\dots\dots\dots\dots\dots (5.14)$$

4. When t=0, $r_{wh}^{0} = r_w = 0.328\ ft$.

5. At every time step there is a new interstitial velocity. The first step is calculated at t = 0:

$$v_i^0 = \frac{Q_i}{2\pi r_w h \emptyset} \ \dots\dots\dots\dots\dots\dots\dots\dots\dots\dots\dots\dots\dots\dots\dots\dots\dots\dots\dots\dots (5.15)$$

$$v_i^0 = \frac{1\ bpm}{2\pi(0.328\ ft)(100 ft)(0.3)} \frac{5.615\ ft^3}{1\ bbl} \frac{30.48\ cm}{1\ ft} = 2.77\ cm/min \ \dots\dots (5.16)$$

6. At every step there is a new wormhole propagation velocity. This first step is calculated at t = 0:

$$v_{wh} = \frac{dr_w}{dt} = \left(\frac{v_i}{PV_{bt,opt}}\right) \times \left(\frac{v_i}{v_{i,opt}}\right)^{-\gamma} \times \left\{1 - exp\left[-4\left(\frac{v_i}{v_{i,opt}}\right)^2\right]\right\}^2 \ \dots\dots\dots\dots\dots (5.17)$$

$$v_{wh} = \left(\frac{2.77\ \frac{cm}{min}}{0.5}\right) \times \left(\frac{2.77\ \frac{cm}{min}}{1.5\ \frac{cm}{min}}\right)^{-1/3} \times \left\{1 - exp\left[-4\left(\frac{2.77\ \frac{cm}{min}}{1.5\ \frac{cm}{min}}\right)^2\right]\right\}^2$$

$$* \frac{1\ ft}{30.48\ cm} = 0.237\ \frac{ft}{min} \ \dots\dots\dots\dots\dots\dots\dots\dots\dots\dots\dots\dots\dots\dots\dots\dots (5.18)$$

7. The new radius of wormhole propagation is calculated as:

$$r_{wh}^{n+1} = r_{wh}^{n} + v_{wh}^{n} \Delta t \ \dots\dots\dots\dots\dots\dots\dots\dots\dots\dots\dots\dots\dots\dots\dots\dots\dots\dots\dots\dots\dots (5.19)$$

$$0.352\ ft = 0.328\ ft + 0.148\ \frac{ft}{min}\ (0.1) \quad \ldots\ldots\ldots\ldots\ldots\ldots\ldots\ldots\ldots\ldots\ldots\ldots\ldots \quad (5.20)$$

8. At every time step there is a new interstitial velocity. The second step is calculated at t = 0.1:

$$v_i^1 = \frac{Q_i}{2\pi r_w h \emptyset} \quad \ldots\ldots\ldots\ldots\ldots\ldots\ldots\ldots\ldots\ldots\ldots\ldots\ldots\ldots\ldots\ldots\ldots \quad (5.21)$$

$$v_i^0 = \frac{1\ bpm}{2\pi(0.343\ ft)(100 ft)(0.3)}\ \frac{5.615\ ft^3}{1\ bbl}\ \frac{30.48\ cm}{1\ ft} = 2.58\ cm/m \ \ldots \ (5.22)$$

9. At every time step there is a new wormhole propagation velocity. This second step is calculated at t = 0.1:

$$v_{wh} = \frac{dr_w}{dt} = \left(\frac{v_i}{PV_{bt,opt}}\right) \times \left(\frac{v_i}{v_{i,opt}}\right)^{-\gamma} \times \left\{1 - exp\left[-4\left(\frac{v_i}{v_{i,opt}}\right)^2\right]\right\}^2 \ \ldots\ldots\ldots\ldots \ (5.23)$$

$$v_{wh} = \left(\frac{2.65\ \frac{cm}{min}}{0.5}\right) \times \left(\frac{2.65\ \frac{cm}{min}}{1.5\ \frac{cm}{min}}\right)^{-1/3} \times \left\{1 - exp\left[-4\left(\frac{2.65\ \frac{cm}{min}}{1.5\ \frac{cm}{min}}\right)^2\right]\right\}^2$$

$$* \frac{1\ ft}{30.48\ cm}$$

$$= 0.226\ \frac{ft}{min} \quad \ldots\ldots\ldots\ldots\ldots\ldots\ldots\ldots\ldots\ldots\ldots\ldots\ldots\ldots\ldots\ldots \quad (5.24)$$

10. Repeat time steps until the total time reaches 238.1 minutes. At 238.1 minutes 100 gal/ft. in total injection volume is reached. The plot is shown in **Figure 5.2.**

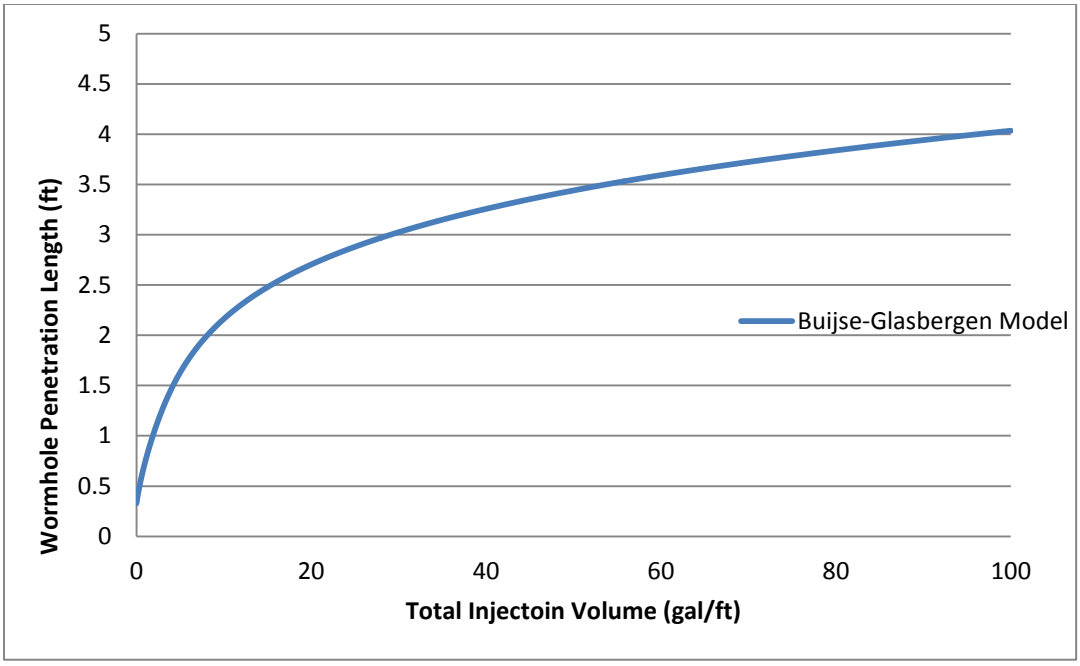

Figure 5.2: Wormhole Propagation Plot with Buijse-Glasbergen Model

5.3 Furui Model Calculation for Wormhole Propagation

For the Furui model the same lab results shown in **Table 5.2** is also used**. Table 5.4** shows the assumed data**:**

Table 5.4: Additional Assumed Data Values

r_w	0.328 ft
ϕ	0.3
Injection acid volume	100 gal/ft
Injection rate	1 bpm
h	100 ft
L_{core}	6 inches
Density of 15% HCl	1.07 g/cm^3
Chalk Density	2.71 g/cm^3
Acid Dissolving Power β_{15} for 15% HCl Solution	0.21 g $CaCO_3$/g 15% HCl
M_{wh}	6
a_z	0.75
γ	1/3

Steps to obtain the wormhole propagation plot:

1. In order to obtain total time to have a total injection volume of 100 gal/ft, the following equation is used:

$$total\ injection\ time = \frac{total\ injection\ volume * \frac{1\ ft^3}{7.48\ gal}}{\frac{q}{h} * 5.615\ \frac{ft^3}{bbl}} \ldots\ldots\ldots\ldots\ldots\ldots\ldots (5.25)$$

$$total\ injection\ time = \frac{100\ \frac{gal}{ft} * \frac{1\ ft^3}{7.48\ gal}}{\frac{1\frac{bbl}{min}}{100\ ft} * 5.615\ \frac{ft^3}{bbl}} = 238.094\ min \quad \ldots\ldots\ldots\ldots\ldots\ldots (5.26)$$

2. Choose Δt. Choosing this value is dependent on how accurate the wormhole propagation plot needs to be.
3. At every time step there is a new injection volume. The first time step is calculated at t = 0:

$$current\ injection\ volume = \frac{total\ injection\ volume}{total\ injection\ time} * current\ injection\ time \ldots\ldots\ldots\ldots (5.27)$$

$$current\ injection\ volume = \frac{100\ \frac{gal}{ft}}{238.1\ min} * 0\ \text{min} = 0\ \frac{gal}{ft} \quad \ldots\ldots\ldots\ldots\ldots\ldots\ldots\ldots\ldots\ldots\ldots\ldots (5.28)$$

4. When t=0, $r_{wh}^0 = r_w = 0.328\ ft$.
5. At every time step there is a new tip interstitial velocity. The first time step is calculated at t = 0:

$$v_{i,tip} = \frac{q}{\phi * h * \sqrt{\pi *\ m_{wh}}} * \left[(1 - a_z) * \frac{1}{\sqrt{d_{e,wh} *\ r_{wh}}} +\ a_z \left(\frac{1}{d_{e,wh}}\right)\right] \ldots\ldots\ldots (5.29)$$

Where, $d_{e,wh}$ is given by:

$$d_{w,wh} = d_{core} *\ N_{AC} *\ PV_{bt,opt} \quad \ldots\ldots\ldots\ldots\ldots\ldots\ldots\ldots\ldots\ldots\ldots\ldots\ldots\ldots\ldots\ldots\ldots\ldots\ldots (5.30)$$

N_{AC} is calculated using this equation:

$$N_{Ac,HCL} = \frac{\phi *\ \beta_{HCl} *\ C_{HCl}^0 *\ \rho_{acid}}{(1 -\ \phi_0) *\ V_F^0 *\ \rho_F} \quad \ldots\ldots\ldots\ldots\ldots\ldots\ldots\ldots\ldots\ldots\ldots\ldots\ldots\ldots\ldots\ldots\ldots\ldots\ldots (5.31)$$

The dissolving power is given by the following equation introduced by Williams, Gidley, and Schechter (1979):

$$\beta = \frac{V_{mineral} * MW_{mineral}}{V_{Acid} * MW_{acid}} \quad \ldots \quad (5.32)$$

For the reaction between 100% HCl and $CaCO_3$,

$$\beta_{100} = \frac{1 * 100.1 \frac{mass}{mole}}{2 * 36.5 \frac{mass}{mole}} = 1.37 \frac{lb_m CaCO_3}{lb_m HCl} \quad \ldots \quad (5.33)$$

Multiplying the dissolving power by 0.15 for 15 wt% HCl we have:

$$0.15 * 1.37 \frac{lb_m CaCO_3}{lb_m HCl} = 0.21 \frac{lb_m CaCO_3}{lb_m HCl} \quad \ldots \quad (5.34)$$

$$N_{Ac,HCL} = \frac{0.3 * 0.21 * 1.07 \frac{g}{cm^3}}{(1 - 0.3) * 2.71 * \frac{g}{cm^3}} = 0.035 \quad \ldots \quad (5.35)$$

$D_{e,,wh}$ is calculated with the acid capacity number.

$$d_{e,wh} = \frac{1\ in}{12 \frac{in}{ft}} * 0.035 * 0.25 = 0.00073\ ft \quad \ldots \quad (5.36)$$

$$v_{i,tip} = \frac{1 \frac{bbl}{min}}{\phi * h * \sqrt{\pi * m_{wh}}} * \left[(1 - 0.75) * \frac{1}{\sqrt{d_{e,wh} * r_{wh}}} + a_z \left(\frac{1}{d_{e,wh}}\right)\right] \quad \ldots \quad (5.37)$$

$$v_{i,tip} = \frac{1 \frac{bbl}{min}}{0.3 * 100 * \sqrt{\pi * 6}} * \frac{5.615\ ft^3}{1\ bbl} \left[(1 - 0.75) * \frac{1}{\sqrt{0.00073 * 0.328}} + a_z \left(\frac{1}{0.00073}\right)\right] * \frac{30.48\ cm}{1\ ft} = 1373.12 \frac{cm}{min} \quad \ldots \quad (5.38)$$

6. At every step there is a new wormhole propagation velocity. This first step is calculated at t = 0:

$$v_{wh}^{n} = v_{i,tip} * N_{Ac} * \left(\frac{v_{i,tip} * PV_{bt,opt} * N_{Ac}}{v_{i,opt}}\right)^{-\gamma} * \left\{1 - \exp\left(-4 * \left(\frac{v_{i,tip} * PV_{bt,opt} * N_{Ac} * L_{core}}{v_{i,opt}}\right)^{2}\right)\right\}^{2} \quad \ldots\ldots\ldots (5.39)$$

$$v_{wh}^{n} = 1373.12\ \frac{cm}{min} * 0.035 * \left(\frac{1373.12\ \frac{cm}{min} * 0.25 * 0.035}{0.77\ \frac{cm}{min}}\right)^{-\frac{1}{3}} * \left\{1 - \exp\left(-4 * \left(\frac{1373.12\ \frac{cm}{min} * 0.25 * 0.035 * 6\ in * 2.54\ \frac{cm}{inch}}{0.77\ \frac{cm}{min} * 0.328\ ft * 30.48\ \frac{cm}{ft}}\right)^{2}\right)\right\}^{2} * \frac{1\ ft}{30.48\ cm} = 0.63\ \frac{ft}{min} \quad \ldots\ldots\ldots\ldots\ldots\ldots\ldots\ldots\ldots\ldots\ldots\ldots\ldots\ldots\ldots\ldots\ldots (5.40)$$

7. The new radius of wormhole propagation is calculated as:

$$r_{wh}^{n+1} = r_{wh}^{n} + v_{wh}^{n}\Delta t \quad \ldots\ldots\ldots\ldots\ldots\ldots\ldots\ldots\ldots\ldots\ldots\ldots\ldots\ldots\ldots\ldots\ldots\ldots\ldots\ldots\ldots\ldots\ldots\ldots\ldots\ldots\ldots\ldots\ldots\ldots (5.41)$$

$$0.391\ ft = 0.328\ ft + 0.63\ \frac{ft}{min}\ (0.1) \quad \ldots\ldots\ldots\ldots\ldots\ldots\ldots\ldots\ldots\ldots\ldots\ldots\ldots\ldots\ldots\ldots\ldots\ldots\ldots\ldots\ldots\ldots\ldots\ldots\ldots\ldots\ldots\ldots\ldots\ldots (5.42)$$

8. At every time step there is a new tip interstitial velocity. The second step is calculated at t = 0.1:

$$v_{i,tip} = \frac{1\frac{bbl}{min}}{\phi * h * \sqrt{\pi * m_{wh}}} * [(1 - 0.75) * \frac{1}{\sqrt{d_{e,wh} * r_{wh}}} + a_z \left(\frac{1}{d_{e,wh}}\right)] \ldots\ldots\ldots\ldots\ldots\ldots\ldots\ldots\ldots\ldots\ldots\ldots\ldots\ldots\ldots\ldots\ldots\ldots (5.43)$$

$$v_{i,tip} = \frac{1\frac{bbl}{min}}{0.3 * 100 * \sqrt{\pi * 6}} * \frac{5.615\ ft^3}{1\ bbl} \left[(1 - 0.75) * \frac{1}{\sqrt{0.00073 * 0.391}} + a_z \left(\frac{1}{0.00073}\right)\right] * \frac{30.48\ cm}{1\ ft}$$

$$= 1371.34\ \frac{cm}{min} \ldots\ldots\ldots\ldots\ldots\ldots\ldots\ldots\ldots\ldots\ldots\ldots\ldots\ldots\ldots\ldots\ldots\ldots\ldots\ldots (5.44)$$

9. At every time step there is a new wormhole propagation velocity. This second step is calculated at t = 0.1:

$$v_{wh}^n = v_{i,tip} * N_{Ac} * \left(\frac{v_{i,tip} * PV_{bt,opt} * N_{Ac}}{v_{i,opt}}\right)^{-\gamma} * \left\{1 - \exp\left(-4 * \left(\frac{v_{i,tip} * PV_{bt,opt} * N_{Ac} * L_{core}}{v_{i,opt}}\right)^2\right)\right\}^2 \ldots\ldots\ldots\ldots\ldots\ldots\ldots\ldots\ldots\ldots (5.45)$$

v_{wh}^{n}

$$= 1371.34\ \frac{cm}{min} * 0.035$$

$$* \left(\frac{1371.34\ \frac{cm}{min} * 0.25 * 0.035}{0.77\frac{cm}{min}} \right)^{-\frac{1}{3}} * \left\{ 1 \right.$$

$$\left. - \exp\left(-4 * \left(\frac{1371.34\ \frac{cm}{min} * 0.25 * 0.035 * 6\ in * 2.54\ \frac{cm}{inch}}{0.77\frac{cm}{min} * 0.3911\ ft * 30.48\ \frac{cm}{ft}} \right)^2 \right) \right\}^2 * \frac{1\ ft}{30.48\ cm}$$

$$= 0.63\ \frac{ft}{min} \quad \ldots\ldots\ldots\ldots\ldots\ldots (5.46)$$

10. Repeat time steps until total time of 238.1 minutes is reached. At 238.1 minutes 100 gal/ft. in total injection volume is reached. The plot is shown in **Figure 5.3.**

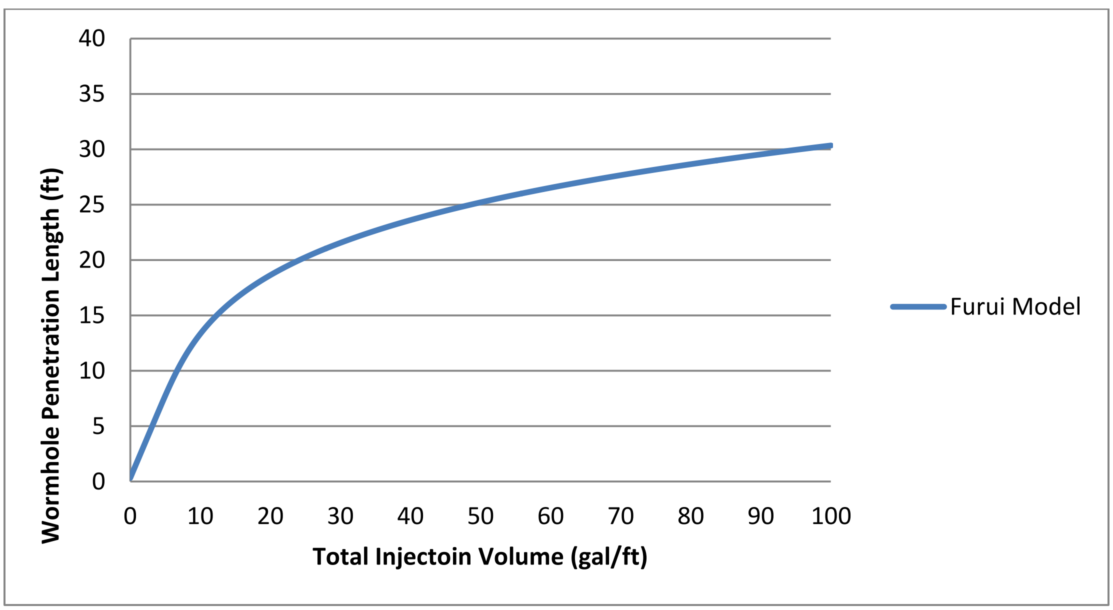

Figure 5.3: Wormhole Propagation Plot with Furui Model

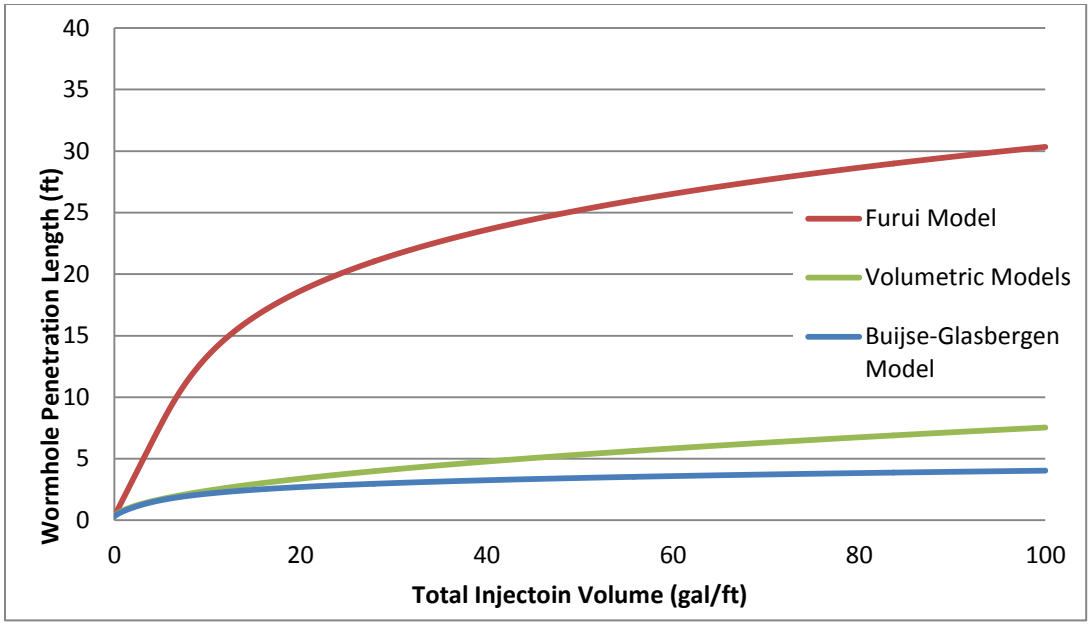

Figure 5.4: Comparison of the Three Models

In **Figure 5.4** the three different models are plotted on one plot. The Furui model gives a much higher wormhole penetration length at every time step than both the volumetric model and Buijse-Glasbergen models.

CHAPTER VI

CONCLUSION AND RECOMMENDATIONS

In this research, 3 sets of experiments were run. The homogenous cores that were run were 4 inches diameter by 4 inches, 6 inches, and 8 inches length. The following conclusions were made based on these experiments:

- The optimum acid injection rate depends on the core length and radius.
- When the core reaches a certain length, the optimum interstitial velocity becomes independent of the core length due to the dominant wormhole being formed.
- When the core length reaches a certain value, the optimum acid injection rate is independent of the core radius given that the core radius is large enough to comprise the early effects of wormhole competition.

Further work can be done on the effect of core geometries on wormhole propagation:

- Conduct experiments using dolomite to observe if same geometry effects apply when the mineralogy is different.
- Conduct experiments at high temperature to observe the effect of core geometry with changing temperature.
- Conduct experiments using different acid concentration to observe the effect of core geometry on various acid concentrations.

REFERENCES

Bazin, B. 2001. From Matrix Acidizing to Acid Fracturing: A Laboratory Evaluation of Acid/Rock Interactions. *SPE Production & Facilities* **16** (1): 22-29.

Buijse, M.A. 2000. Understanding Wormholing Mechanisms Can Improve Acid Treatments in Carbonate Formations. *SPE Production & Operations* **15** (3): 168-175. doi: 10.2118/65068-pa.

Buijse, M.A. and Glasbergen, G. 2005. A Semiempirical Model to Calculate Wormhole Growth in Carbonate Acidizing. Paper SPE 96892 presented at the SPE Annual Technical Conference and Exhibition, Dallas, Texas, 10/09/2005. doi: 10.2118/96892-ms.

Daccord, G., Touboul, E., and Lenormand, R. 1989. Carbonate Acidizing: Toward a Quantitative Model of the Wormholing Phenomenon. *SPE Production Engineering* **4** (1): 63-68. doi: 10.2118/16887-pa.

Dong K. 2012. Experimental Investigation For the Effect of the Core Length On the Optimum Acid Flux in Carbonate Acidizing. Master of Science Thesis, Texas A&M University, College Station.

Fredd, C.N. and Fogler, H.S. 1999. Optimum Conditions for Wormhole Formation in Carbonate Porous Media: Influence of Transport and Reaction. *SPE Journal* **4** (3): 196-205. doi: 10.2118/56995-pa.

Frick, T.P., Mostofizadeh, B., and Economides, M.J. 1994. Analysis of Radial Core Experiments for Hydrochloric Acid Interaction with Limestones. Paper Copyright 1994, SPE 27402 presented at the SPE Formation Damage Control Symposium, Lafayette, Louisiana, 02/07/1994. doi: 10.2118/27402-ms.

Furui, K., Burton, R.C., Burkhead, D.W., Abdelmalek, N.A., Hill, A.D. et al. 2010. A Comprehensive Model of High-Rate Matrix Acid Stimulation for Long Horizontal Wells in Carbonate Reservoirs. Paper SPE 134265-MS presented at the SPE Annual Technical Conference and Exhibition, Florence, Italy, 09/19/2010. doi: 10.2118/134265-ms.

Ghosh V. 2013. Matrix Acidizing Parallel Core Flooding Apparatus. Master of Science Thesis, Texas A&M University, College Station.

Grabski, E.R. 2012. Matrix Acidizing Core Flooding Apparatus: Equipment and Procedure Description. Master of Science Thesis, Texas A&M University, College Station.

Hill, A.D., Zhu, D., and Wang, Y. 1995. The Effect of Wormholing on the Fluid –Loss Coefficient in Acid Fracturing. *SPE Prod& Fac.* **10** (4): 257-264. SPE-27403-PA.

Hoefner, M.L. and Fogler, H.S. 1987. Role of Acid Diffusion in Matrix Acidizing of Carbonates. *SPE Journal of Petroleum Technology* **39** (2): 203-208. doi: 10.2118/13564-pa.

Hoefner, M.L. and Fogler, H.S. 1989. Fluid-Velocity and Reaction-Rate Effects During Carbonate Acidizing: Application of Network Model. *SPE Production Engineering* **4** (1): 56-62. doi: 10.2118/15573-pa.

Hung, K.M., Hill, A.D., and Sepehrnoori, K. 1989. A Mechanistic Model of Wormhole Growth in Carbonate Matrix Acidizing and Acid Fracturing, *JPT* (January 1989) **59**; Trans., AIME, 287.

Mostofizadeh, B. and Economides, M.J. 1994. Optimum Injection Rate from Radial Acidizing Experiments. Paper SPE 28547 presented at the SPE Annual Technical Conference and Exhibition, New Orleans, Louisiana, 09/25/1994. doi: 10.2118/28547-ms.

Smits, F.C.M. 2001. Wormholing: The Key to Acid Stimulation Treatments in Carbonate Reservoirs. Master of Science Thesis. Utrecht University. Utrecht, The Netherlands.

Talbot, M.S. and Gdanski, R.D. 2008. Beyond the Damkohler Number: A New Interpretation of Carbonate Wormholing. Paper SPE 113042 presented at the Europec/EAGE Conference and Exhibition, Rome, Italy, 06/09/2008. doi: 10.2118/113042-ms.

Wang, Y., Hill, A.D., and Schechter, R.S. 1993. The Optimum Injection Rate for Matrix Acidizing of Carbonate Formations. Paper SPE 26578 presented at the SPE Annual Technical Conference and Exhibition, Houston, Texas, 10/03/1993. doi: 10.2118/26578-ms.

Williams, B.B., Gidley, J.L., and Schechter, R.S. 1979. Acidizing Fundamentals, Society of Petroleum Engineers, Richardson, TX.